

**UNIVERSITY OF GAZIANTEP
GRADUATE SCHOOL OF
NATURAL & APPLIED SCIENCES**

FLOW FIELD AROUND TALL BUILDINGS

**M. Sc. THESIS
IN
CIVIL ENGINEERING**

**BY
OMAR A. MAHMOOD
JANUARY 2014**

Flow Field around Tall Buildings

**M.Sc. Thesis
In
Civil Engineering
University of Gaziantep**

**Supervisor
Assist. Prof. Dr. Mehmet İshak YÜCE**

**By
OMAR A. MAHMOOD
JANUARY 2014**

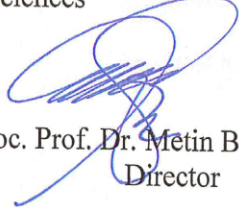
© 2014 [OMAR A. MAHMOOD]

T.C.
UNIVERSITY OF GAZIANTEP
GRADUATE SCHOOL OF
NATURAL & APPLIED SCIENCES
CIVIL ENGINEERING DEPARTMENT

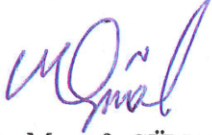
Name of the thesis: Flow Field around Tall Buildings

Name of the student: OMAR A. MAHMOOD
Exam date: 31/01/2014

Approval of the Graduate School of Natural and Applied Sciences


Assoc. Prof. Dr. Metin BEDİR
Director

I certify that this thesis satisfies all the requirements as a thesis for the degree of Master of Science.


Prof. Dr. Mustafa GÜNAL
Head of Department

This is to certify that we have read this thesis and that in our opinion it is fully adequate, in scope and quality, as a thesis for the degree of Master of Science.


Assist. Prof. Dr. Mehmet İshak YÜCE
Supervisor



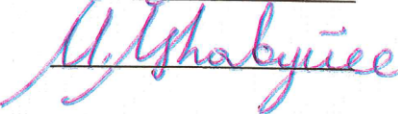
Examining Committee Members

Signature

Prof. Dr. Mustafa GÜNAL

Assoc. Prof. Dr. Murat PALA

Assist. Prof. Dr. Mehmet İshak YÜCE

I hereby declare that all information in this document has been obtained and presented in accordance with academic rules and ethical conduct. I also declare that, as required by these rules and conduct, I have fully cited and referenced all material and results that are not original to this work.

OMAR A. MAHMOOD

ABSTRACT

FLOW FIELD AROUND TALL BUILDINGS

MAHMOOD, OMAR A.

M.Sc. in Civil Engineering

Supervisor: Assist. Prof. Dr. Mehmet İshak YÜCE

Alongside vertical loads, tall buildings are subjected to lateral loads such as wind and seismic loads. Under the action of wind flow, tall buildings oscillate simultaneously both in the direction of wind and orthogonal to the direction of wind. In some cases even torsional effect may occur. Slender and lightweight modern tall structures, which have less stiffness and damping property, are more sensitive and prone to the dynamic serviceability problems. High-rise buildings are bluff bodies submerged in air flow field, which are subjected to various forces due to pressure and velocity changes. The interaction between wind and tall buildings are the great challenge depends on the exposure type of wind, topography, interference with another buildings, wind direction and geometrical shape of the buildings.

In this study, three different building plan area shapes; basic rectangle, single corner-recession and double corner-recession were studied by Computational Fluid Dynamics (CFD). In the simulations k-e turbulence closure model was employed with wind velocity of 26 m/s. The results obtained from the simulation analyses of rectangular shaped plan area building model was compared with a number of widely used codes and showed good agreement. Both the along wind and across wind base shear forces and base bending moments acting on the buildings were observed to be affected from the shape of the plan areas of the models. The values of these forces were noted to be the highest for the basic rectangular shape while they were lowest for the double corner-recession shape.

Keywords: Tall Buildings, Wind Effect, Computational Fluid Dynamics, CFD, ANSYS FLUENT

ÖZET

YÜKSEK YAPILAR İN ETRAFINDAKİ AKİM ALANI

MAHMOOD, OMAR A.

M.Sc. in Civil Engineering

Supervisor: Assist. Prof. Dr. Mehmet İshak YÜCE

Yüksek binalar, düşey yükleri yanısıra, rüzgar ve deprem yükleri gibi yatay yüklerde maruz kalırlar. Rüzgar akımının etkisindedir kalan yüksek yapılar, rüzgar yönünde ve rüzgar yönüne dik olacak şekilde titreşime maruz kalırlar. Bazı durumlarda burulma etkisi dahi ortaya çıkabilir. Daha az sertlik ve sönümleme özelliğine sahip olan ince ve hafif, modern yüksek yapılar hizmet verebilirlik problemlerine karşı daha hassastırlar. Yüksek binalar, hava akım alanı içine gömülmüş kaba yapılardır ve dolayısı ile basınç ve akım hızında meydana gelen değişikliklerden ötürü çeşitli kuvvetlere maruz kalırlar. Rüzgar ve yüksek yapılar arasındaki etkileşim, rüzgar yönü, binaların geometrik şekli, topografya ve etraftaki binalar konumu gibi faktörlerden ciddi oranda etkilendir.

Bu çalışmada, basit dikdörtgen, tek girinti köşeli dikdörtgen ve çift girinti köşeli dikdörtgen gibi üç farklı bina plan alanı şekli hesaplamalı akışkanlar dinamiği (CFD) kullanılarak incelenmiştir. Simülasyonlarda k-ε türbülans modeli kullanıldı ve rüzgar hızı 26 m/s olarak seçildi. Basit dikdörtgen şeklindeki plan alanlı bina modelinin simülasyon analizlerinden elde edilen sonuçlar yaygın olarak kullanılan kodlar ile karşılaştırıldı ve sonuçların bir biri ile iyi uyum gösterdiği tespit edildi. Rüzgar yönünde ve rüzgara dik yönde meydana gelen taban kesme kuvvetleri ve eğilme momentleri bina modellerin plan alanlarının şeklinden etkilendiği tespitine varıldı. Bu kuvvetlerin, çift girinti köşeli dikdörtgen şekil için en düşük iken basit dikdörtgen şekli için en yüksek olduğu kaydedildi .

Anahtar Kelimeler: Yüksek Binalar, Rüzgar Etkisi, Hesaplamalı Akışkanlar Dinamiği, CFD, ANSYS FLUENT.

ACKNOWLEDGMENT

I express my sincere gratitude to my supervisor Assist. Prof. Dr. Mehmet Ishak YUCE for his guidance and invaluable advice during this research. It was my pleasure to work under his supervision. I would not have been able to complete this work without his guidance and direction.

I would like to thank to my relatives for their help, without their support this research project could not have been possible.

TABLE OF CONTENTS

CONTENTS	Page
ABSTRACT.....	vi
ÖZET.....	vii
ACKNOWLEDGMENT.....	vii
TABLE OF CONTENTS.....	viii
LIST OF FIGURES.....	xi
LIST OF TABLES.....	xv
LIST OF SYMBOLS / ABBREVIATIONS.....	xvi
CHAPTER 1.....	1
INTRODUCTION.....	1
1.1 Atmosphere.....	1
1.2 Winds.....	2
1.2.1 Pressure gradient.....	4
1.2.2 Rotation of the earth.....	4
1.2.3 Friction of the earth.....	4
1.3 Bluff Body Aerodynamics.....	4
1.3.1 Along-wind Load.....	6
1.3.2 Across-wind Load.....	7
1.3.3 Torsional Load.....	7
1.4 Importance of Wind Load on Tall Structures.....	8
1.5 Objectives and Scope of the Work.....	11
1.6 Structure of Thesis.....	11
CHAPTER 2.....	13
LITERATURE REVIEW.....	13
2.1 General (Introduction).....	13
2.2 Factors Affecting Wind Load.....	13
2.2.1 Topography and Roughness of the Surrounding Terrain.....	13
2.2.2 Direction of Wind.....	14

2.2.3 The Buildings Dynamic Characteristics	14
2.2.4 Building Shape.....	14
2.2.5 Interference Effects.....	15
2.3 Approach Methods for Estimating Wind Loads on Tall Buildings.....	15
2.3.1 Code Estimated Wind Loads	15
2.3.2 Wind Tunnel Test	16
2.3.2.1 High Frequency Force Balance (HFFB)	17
2.3.2.2 High Frequency Pressure Integration (HFPI)	17
2.3.2.3 Aero-elastic Model Studies	18
2.3.3 Computational Fluid Dynamics (CFD)	19
2.4 History of the Subject.....	19
2.4.1 Dynamic Analysis of Wind Force	20
2.4.2 Analytical Work.....	24
2.4.3 CFD simulation.....	29
CHAPTER 3	33
METHODOLOGY	33
3.1 Introduction	33
3.2 Turbulence.....	33
3.2.1 k- ϵ models.....	36
3.2.1.1 The realizable k-epsilon model	37
3.3 Modeling and Simulation Procedure	38
3.3.1 Pre-processing.....	38
3.3.1.1 Creating the model and defining the geometry	39
3.3.1.2 Creating the boundary layer and meshing.....	41
3.3.2 Simulation.....	44
3.3.2.1 The physical procedure	44
3.3.2.2 Defining the fluid properties	44
3.3.2.3 Specification of boundary conditions	44
3.3.3 Initialization and solution	45
3.3.4 Post-processing	46
CHAPTER 4	47
RESULTS AND DISCUSSIONS	47
4.1 Velocity profiles	47

4.2 Velocity streamlines	49
4.3 Velocity vectors.....	50
4.4 Velocity contours	53
4.4.1 Horizontal velocity contour	53
4.4.2 Vertical velocity contours.....	53
4.5 Pressure on the Building Faces.....	56
4.6 Base Shear and Base Bending Moments	59
CHAPTER 5	65
CONCLUSIONS.....	65
REFERENCES.....	68
Appendix A	77

LIST OF FIGURES

FIGURES	Page
Figure 1.1 Temperature profile T , density ρ and pressure P in the mean atmosphere	2
Figure 1.2 Flow field around bluff bodies.....	6
Figure 1.3 Tacoma bridge collapse due to wind effect	9
Figure 1.4 Ferry-bridge reinforced concrete cooling towers collapse due to wind.....	10
Figure 3.1 The whole domain of double recession building	39
Figure 3.2 Top view of the domain of the double recession building model.....	40
Figure 3.3 Side view of the domain of the double recession building model	40
Figure 3.4 Front view of the domain of the double recession building model.....	40
Figure 3.5 Meshing of the domain	41
Figure 3.6 Mesh metric of the building in double recession model	42
Figure 3.7 The top view of rectangular building model with the mesh	43
Figure 3.8 Side view of rectangular building model with the mesh	43
Figure 3.9 The vertical cross-section of rectangular building model with the mesh	43
Figure 3.10 The residuals vs. number of iterations for rectangular building model.....	45

Figure 4.1 Vertical velocity profiles from the center of the rectangular building model	48
Figure 4.2 Vertical velocity profiles from the center of the single recession building model	48
Figure 4.3 Vertical velocity profiles from the center of the double recession building model	48
Figure 4.4 Horizontal velocity streamlines in the domain at height 50 m from ground for double recession building model	49
Figure 4.5 Vertical velocity streamlines in the domain at the center of the double recession building model.....	50
Figure 4.6 Horizontal velocity vectors for rectangular building at height of 50 m from the ground.....	51
Figure 4.7 Horizontal velocity vectors for single recession at height of 50 m from the ground.....	51
Figure 4.8 Horizontal velocity vectors in double recession building at height of 50 m from ground.	51
Figure 4.9 Horizontal velocity vectors for rectangular at height of 50 m from the ground near building.....	52
Figure 4.10 Horizontal velocity vectors for single recession at height of 50 m from the ground near building	52
Figure 4.11 Horizontal velocity vectors for double recession at height of 50 m from the ground near building	52
Figure 4.12 The velocity distribution at height of 50 m from ground for rectangular building	54
Figure 4.13 The velocity distribution at height of 50 m from ground for single recession building	54

Figure 4.14 The velocity distribution at height of 50 m from ground for double recession building.....	54
Figure 4.15 Vertical velocity contours from the center of rectangular building	55
Figure 4.16 Vertical velocity contours from the center of single recession building	55
Figure 4.17 Vertical velocity contours from the center of double recession building	55
Figure 4.18 Pressure contour on windward and leeward faces of the double recession building.....	56
Figure 4.19 Pressure distribution on windward faces of all three building models	58
Figure 4.20 Pressure distribution on leeward faces of all three building models	58
Figure 4.21 Base shear in the along wind direction by different codes and CFD Simulation	60
Figure 4.22 Base bending moment in the along wind direction by different codes and CFD Simulation.....	60
Figure 4.23 Base shear in the across wind direction by different codes and CFD Simulation	61
Figure 4.24 Base bending moment in the across wind direction by different codes and CFD Simulation.....	61
Figure 4.25 Base shear in the along wind direction different shapes of buildings by CFD Simulation.....	62
Figure 4.26 Base bending moment in the along wind direction different shapes of buildings by CFD Simulation.....	63

Figure 4.27 Base shear in the across wind direction different shapes of buildings by CFD Simulation.....	64
Figure 4.28 Base bending moment in across wind direction different shapes of buildings by CFD Simulation	64

LIST OF TABLES

TABLES	Page
Table 3.1 Dimensions of whole domain.....	41
Table 3.2 Dimensions of the three alternative building types.....	41
Table 3.3 Properties of air	44
Table 3.4 The boundary conditions of the domain.....	45

LIST OF SYMBOLS / ABBREVIATIONS

2D	Two Dimensional
3D	Three Dimensional
ABL	Atmospheric boundary layer
ASCE	American Society of Civil Engineers
CFD	Computational Fluid Dynamics
C_p	Surface pressure distribution
d	Is the across-wind characteristic length
D.O.F	Degree of freedom
DNS	Direct numerical simulation
ESDU	Engineering Science Data Unit
EVM	Eddy Viscosity Modeling
HFFB	High Frequency Force Balance
HFPI	High Frequency Pressure Integration
L	Is the characteristic length

ϵ	Turbulence dissipation energy
K	Turbulence kinetic energy
LES	Large Eddy Simulation
M.D.O.F	Multi degree of freedom
n_s	Is the frequency of the vortex shedding
ρ	Density of air
RMS	Root mean square
RNG	Re-Normalizing Group
T	Temperature
\bar{u}	Mean velocity of the approaching flow
UDF	User defined function
USD	United State dollar
V	Velocity of flow
α	Power law exponent
μ	Dynamic viscosity of the fluid

CHAPTER 1

INTRODUCTION

1.1 Atmosphere

The layers of gases surrounding the planet earth, which are retained by the gravitational forces, is called atmosphere. The atmosphere's main function is to protect the life on earth by absorbing infrared solar radiation and controlling the great temperature changes between night and day which is called the diurnal variations of temperatures. The total mass of the atmosphere is estimated to be around 5×10^{18} kg. About 80% of that mass is located within 11 km altitude of the surface. With increasing altitude the atmosphere's density decreases. However, there is no specific limit between the atmosphere and outer space. Having said that, a figure of 100 km (less than 1.6% of the earth's radius) is usually taken to be the border between the space and atmosphere.

Based on their temperature characteristics and chemical composition the atmosphere can be divided in to several layers. Figure 1.1 shows the entire layers in great details. The temperature relation with altitude is a more complicated profile compare to the density and air pressure in which both decreasing with increasing altitude.

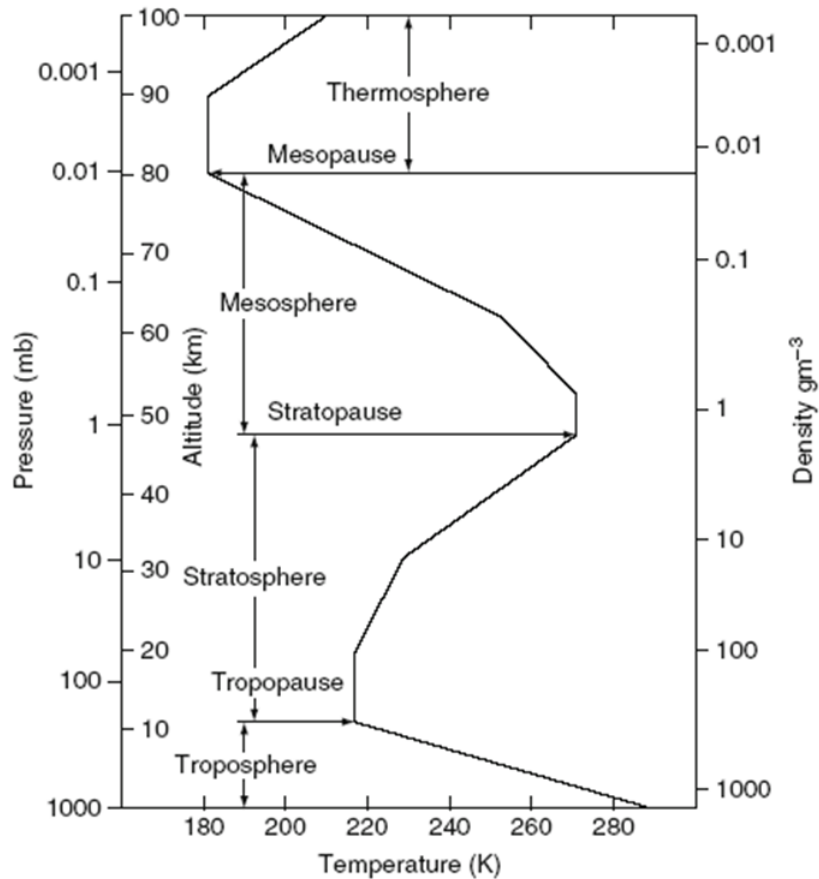


Figure 1.1 Temperature profile T , density ρ and pressure P in the mean atmosphere

1.2 Winds

The horizontal movement of air relative to the earth's surface is called wind. The vertical movement of the air is known as air current. Winds and air currents together comprise a system of circulation in the atmosphere. The earth's gravity and the differential solar heating of earth's atmosphere lead to generating atmospheric circulation.

Air temperature varies because the earth's surface heats up at different rates. Latitude and seasons cause temperature variations. Large bodies of water heat up and cool down at a slower rate than large bodies of land, creating a disparity in the atmosphere above. Since heat decreases with altitude, mountain peaks are cooler than cities at sea level. These are the main causes of differing temperatures of the atmosphere.

The winds can be classified into two main types according to the direction of blowing with respect to the time. The prevailing winds are those types which are blowing in the specific direction throughout the year, and the periodic winds reverse the direction of flow with respect to the time of the year.

Prevailing winds are also called planetary or permanent winds. The winds blow from the high pressure centers to the low pressure centers. These winds tend to deflect under the action of fictitious force induced by the earth's rotation which is called Coriolis force. According to Ferrell's Law the direction of winds are deflected. The main types of prevailing winds are westerlies, tropic (trade) winds and Polar easterlies.

Sea and land breezes, also monsoon winds are considered as periodic types. They are induced by unequal heating of sea and land. Monsoon winds occur seasonally, while the occurrence of land and sea breezes are daily.

There is another type of wind which is named as local winds. Local winds are the result of a variety of causes. The mountain and valley winds follow a daily alteration of direction in a manner like the land and sea breezes. During the day, when slopes are intensely heated by the Sun, the air moves from the valleys upward over rising mountain slopes towards the summits. This is known as valley winds. It decreases the temperature of the areas on higher summits. At night, when the same slopes have been cooled by radiation from ground to the air, the air in the valley moves downwards and reduces the temperature of the valleys. These winds, which respond to the local pressure gradients, are caused by the heating or cooling of the ground. In winter, a cold and dense air may accumulate over highland and flow out upon adjacent lowlands as a strong cold wind. The movement and the speed of winds are

affected by three main factors; friction of the earth, rotation of the earth, pressure gradient.

1.2.1 Pressure gradient

Winds blow from high pressure regions to low pressure regions. Velocity of the wind depends on the pressure gradient, in other words, the wind velocity increases while the difference between atmospheric pressures at two specific points increased and vice versa.

1.2.2 Rotation of the earth

In addition to the pressure gradient, Coriolis force, which is induced by rotation of the earth, is another force to generate winds. This force tends to change the direction of the wind from straight to curved path. In the northern hemisphere winds deflect to their right from their original path, however, in the southern hemisphere they deflect to their left from their original path of motion regardless of the compass direction of the path. The deflection is the least at the equator and the greatest at the poles.

1.2.3 Friction of the earth

Both velocity and angular deflection of winds decrease by the effect of the friction of the earth's surface. Friction has a considerable effect over the forested and mountains areas, nonetheless very small effect over massive ocean surfaces.

1.3 Bluff Body Aerodynamics

Tall buildings under the action of wind are generally treated as prismatic bluff bodies that have various plan dimensions and oscillate in the along wind, across-wind and torsional directions (Lin et al., 2005; Holmes, 2007). Compared to streamlined bodies, where the flow streamlines follow the outlines of the body. Bluff bodies are

characterized by large regions of separated flow, large drag forces and the formation of vortex shedding Roshko (1993). Figure 2.1 is a schematic plan view of the average air flow around a streamlined body and a bluff body with a rectangular cross-section (Roshko 1993; Simiu 1996; Holmes 2007). As indicated in the figure, the separated flow region consists of the outer region, where there are no viscous effects and the inner region, where viscous effects govern. A thin region known as the free shear layer that has complex flow characteristics with high shear and vorticity separates the inner and outer regions Holmes (2007). If the bluff body has a long after-body, the flow may reattach to the surface of the body and will be followed by a second separation point at the corners downstream of the body (Taylor et al. 2011); otherwise the flow will remain separated and generate a large wake at the lee of the body. A separation bubble is formed between the free shear layer and the body from the initial separation point and the reattachment point (Djilali 1992; Taylor et al. 2011). The wake region downstream of the body is characterized by a region with low velocity and turbulent flow Holmes (2007).

The unstable nature of the flow surrounding the bluff body and the turbulent nature of the approaching air flow generate highly fluctuating loads. First, the approaching flow defined as the atmospheric boundary layer has natural turbulence or gustiness often called buffeting. Second, the bluff body itself can generate unsteady flows through separation of flow, reattachment and vortex shedding. Finally, the movement of the body can also generate fluctuating forces also known as the aerodynamic damping, which can be significant for highly flexible vibration-prone aero-elastic structures. The response of a tall building under wind load consists of components in the along-wind, across-wind, and torsional directions, as illustrated in Figure 1.2. The along-wind response of a building is the response of the building parallel to the

direction of wind. The across-wind response is the building's response, which is perpendicular to the direction of wind. The torsional response describes the twisting motion of the building about the vertical axis.

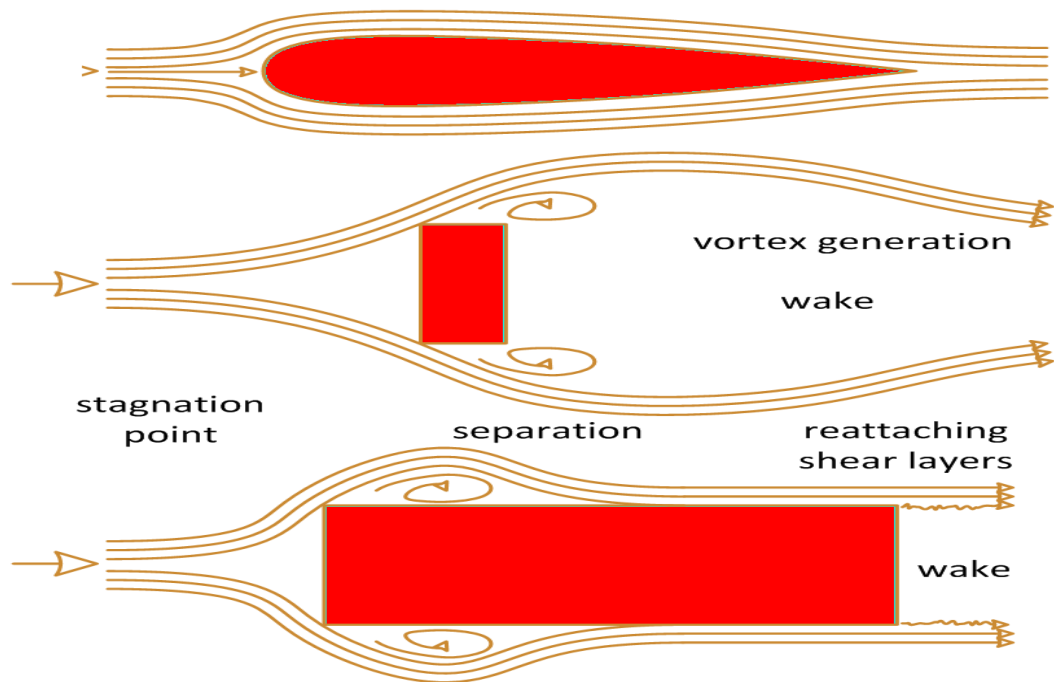


Figure 1.2 Flow field around bluff bodies

1.3.1 Along-wind Load

The along-wind load results from the net pressure fluctuations acting in the direction parallel to the wind. The along-wind response of a tall building is generally considered by applying the quasi-steady theory (Richards and Hoxey, 2004), which assumes that the fluctuating pressure on the windward face of the structure varies directly with the fluctuation of the longitudinal wind velocity. The total along-wind force is the sum of the forces acting on the windward and leeward faces of the structure. The load in the leeward face of the structure is generally caused by the pressure fluctuations in the recirculation region of the wake. The wake recirculation region is highly turbulent but has low velocities, and in turn low pressures.

1.3.2 Across-wind Load

Vortex shedding is the primary mechanism for generating the across-wind response on a bluff body (Davenport, 1966; Lin et al., 2005; Holmes, 2007). Vortex shedding is described as the alternating shedding of vortices from the rolling up of separating shear layers into the wake and is influenced by the turbulence in the approaching flow (Davenport, 1966; Holmes, 2007). The frequency of the alternating forces, i.e. vortex shedding, can be expressed as a non-dimensional value known as the Strouhal number, S_t , (Simiu, 1996; Holmes, 2007) defined as follows;

$$S_t = \frac{n_s d}{\bar{u}} \quad (1.1)$$

where n_s is the frequency of the vortex shedding (i.e. the Strouhal frequency); d is the across-wind characteristic length, i.e. plan dimension perpendicular to the direction of wind, and \bar{u} is the mean velocity of the approaching flow. The forces generated by the shedding of vortices on the structure depend on the turbulence in the flow, the dimensions of the bluff body and the natural frequency of the bluff body Davenport (1966). The across-wind force can be much larger than the along-wind force if the Strouhal frequency is at resonance with the natural frequency of the bluff body within a uniform steady flow Davenport (1966).

1.3.3 Torsional Load

The twisting motion of a bluff body subjected to air flow results from the non-uniform pressure distribution around the wall faces of the bluff body. This mechanism was generally studied through measuring aerodynamic loads in wind tunnel tests and CFD codes on bluff bodies with varying shapes, presence of other interfering bodies and various angles of the approaching flow (Boggs et al. 2000). The pressure distribution around the bluff body can change when the shape of the

bluff body is altered.

1.4 Importance of Wind Load on Tall Structures

Understanding the interaction between wind and structures has always been an important requirement in the field of tall building analysis and design. As tall structures are more prone to lateral wind loads than vertical live and dead loads, designers need to know the distribution of the fluctuating wind pressures on the outer surfaces of the building. This knowledge is needed to calculate the wind forces and moments acting at various levels so that the dynamic response of the structure can be determined. However, the prediction of these quantities in details is usually a challenging task due to the complicated nature of wind patterns developed around structures. Turbulent flow characteristics such as the formation of the shear layer, impingement, separation and vortex shedding, to name a few, all contribute to the complex motion of the structure in space as a result.

Three important failures of the structures concerning wind action are the main point that can be highlighted here. These failures are important landmarks in the art of designing wind and they can be shown here in order of a time scale that they occurred. Consideration to wind action was first taken to the front of the field in 1940 when the Washington State's Tacoma Narrows Bridge (Figure 1.3) distorted under moderate, 64 km/h wind speed and that was the starting point for the engineers to think about this important issue. Later on this example became the most famous example of the effects of wind action on large structures or buildings. Inattention to the vibratory nature of the structure was the main reason for the collapse; the slow but continued winds instigated the bridge to oscillate at its natural frequency, till collapse the amplitude of vibration was increasing. Scott (2001) suggested a wind

tunnel test which later on was implemented for the subsequent design of the bridge.



Figure 1.3 Tacoma bridge collapse due to wind effect

In 1965, the second failure of the three, out of the overall of eight, 122 m reinforced concrete cooling towers happened. It was the Ferry-bridge cooling towers in England (Figure 1.4), this failure also confirmed the dynamic effects of wind on structures, meanwhile at that time most of the designs were considered the wind action as quasi-static Richards (1966). However, wind has a gusty property and in structural design the peak value of its speed has to be considered, not its average wind speed alone, particularly for tall and flexible structure. The main reason for the failures of these towers was reported to be the strong wind gusts as the wind load tension overpowered the dead load compression. Regarding the same failure Armitt (1980) stats that wind load was overblown by the other towers surrounding.

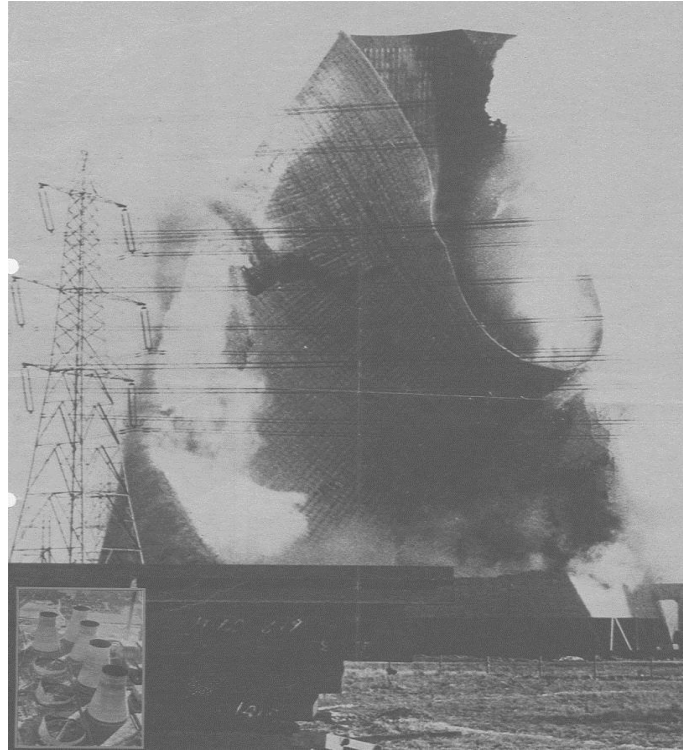


Figure 1.4 Ferry-bridge reinforced concrete cooling towers collapse due to wind

The third failure was Boston's John Hancock Tower. In 1973 the John Hancock tower came across a 121 km/h wind that crashed over 65,000 pounds of double glazing window to the side street. The reason for the failures of the windows was covered up by the involved party's agreement and was never found. In the meantime Campbell (1996) has suggested that the reason for the failure of the window was actually the designs of the window itself. On the other hand the moderate wind speed swayed the towers extensively was causing a discomfort to the higher floors residents. This major issue was not acceptable and was solved by installing two-three hundred tons tuned mass dampers. This new invention was recently used for the Citicorp Tower in New York LeMessurier (1993). After it was found that the towers were prone to failure in the case of heavy wind at cost of five million USD an additional lateral bracing was added to the central core. (Campbell, 1996; Sutro, 2000).

1.5 Objectives and Scope of the Work

This study examines the feasibility of employing CFD in the numerical modeling of wind flow around tall buildings, consequently predicting the flow characteristics around tall buildings. The test configurations consist of three equivalent alternatives cross sectional area, first is rectangular, second is rectangular single recession, and the third one is rectangular double recession each one have 1380 m² with 183 m height. Wind pressure distribution over the model's faces was obtained and the flow characteristic around and downstream of the building was determined. Realizable k-epsilon turbulent model, which is available in ANSYS FLUENT 14.0, was employed.

1.6 Structure of Thesis

This study is divided into 5 chapters. Chapter 1 is about the wind. The introduction to earth's atmosphere and its major layers and boundaries between them in a short-term were given. The main sources that lead to generating winds and the factors affecting on the wind speed and its direction defined. The all wind types even they are permanent or periodic were mentioned. Analysis of the major problems that induced in the tall building structures was done in this chapter. Also the important of the wind loads on the tall structure briefly described, some well-known of the totally or partially structure failures due to wind effect are mentioned. In the end of the chapter the purpose and the scope of the work illustrated, finally the structure of the thesis described.

Chapter 2 contain general sketch of the chapter itself. The main factors that lead to change the effect of the wind loads on tall structures are mentioned. In the chapter provide general information on the approach methods that used in estimating the

wind load on tall buildings. The main approaches are codes, wind tunnel tests, and CFD codes. The detail of historical work which is including experimental, analytical and CFD work was presented. In the chapter the experimental works divided dynamic analysis, pressure measurement, and full scale measurement works that was done in the past time.

Chapter 3 the turbulence definition and its characteristic are described with the popular turbulence model method k- ϵ model especially realizable type. Later the building shapes, its scaled size and its virtual wind tunnel were modeled. Finally the simulation process and detailed information for each step is explained.

In chapter 4 the result of the work and discussion about it was done.

Finally the conclusion and future works were given in chapter 5.

CHAPTER 2

LITERATURE REVIEW

2.1 General (Introduction)

This chapter presents the main factors affecting wind loads on tall buildings. Later the approach methods for estimating wind loads are mentioned. finally a review of relevant literature to bring out the background of the study undertaken in this thesis. The research contributions which have a direct relevance are treated in greater detail. Some of the historical works which have contributed greatly to the understanding of the wind loading on structures are also described. First, a brief review of the historical background is presented. The amount of the literature on the subject has increased rapidly in recent years; particularly to wind such as tall, slender buildings and lightweight Structures. Several of this is available in the proceedings of the conferences which are very helpful to understand the recent developments in wind engineering.

2.2 Factors Affecting Wind Load

2.2.1 Topography and Roughness of the Surrounding Terrain

The terrain topography has an influence on the wind loads. In most of analytical methods the factor of topographic exposure of surrounding terrain for estimating wind loads are taken into account. In wind tunnel test, the surrounding area can create in a scale model, so as to represent the real situation and get the more precise results.

2.2.2 Direction of Wind

In calculating wind loads on the buildings in analytical method assumed that the wind is blowing perpendicular to the face of the building, without considering of the orientation of the building with respect to the wind direction in the side. So as to adjust the estimation wind load for different alignment of the building according to wind direction the factor putting in the calculation, that is called wind directionality factor (Davenport, 1977, Ellingwood et al., 1980). This factor accounts for two effects; first the reduced probability of maximum winds coming from any given direction, and the second reduced probability of the maximum pressure coefficient occurring for any given wind direction.

2.2.3 The Buildings Dynamic Characteristics

Buildings rigidity have an effect on the wind loads especially in the along wind direction. When the building not oscillate under the action of wind In case of stiff buildings like reinforced concrete the effect of wind gusts is neglected in analytical methods. In elastic building cases like light weight steel structures the load increases by the effect of the gusts that produces from oscillation of the building. In analytical methods this effect must be taken into account in calculating pressure, and in CFD and wind tunnel test cases the model must represents the real building, or adding the effect of buildings dynamic characteristics analytically.

2.2.4 Building Shape

The building geometrical shape affects greatly on the wind- structure interaction. Particularly for torsional forces which affecting on the buildings. Codes not valuable for estimating wind loads on the irregular shapes of the buildings, which is tall or slender building. In this case, recommended to estimate the wind load by using the

CFD or wind tunnel test. In popular building shapes and low rise the codes and specifications are workable approach to estimate wind load.

2.2.5 Interference Effects

The wind characteristic in the crowded urban area changed due to existing of many high rise building, which is affected on the each building individually by the effect of the other buildings. The effect of interference is large as established at the 1970's in lawsuit filed by the owners of many buildings in New York City in the neighborhood of the World Trade Center Towers, who observe unusual wind velocity in the pedestrian level and unusual wind pressure on their buildings Kwok (1989) due to the newly constructed Towers.

The CFD and wind tunnel testing is a workable approach to estimating the effect of the surrounding structures. The differences between CFD and wind tunnel test with specification greatly depend on the interference (shielding) effects.

2.3 Approach Methods for Estimating Wind Loads on Tall Buildings

2.3.1 Code Estimated Wind Loads

For many common and simple geometrical building shapes the wind loads can be determine by codes in acceptable level. Advanced wind tunnel testing is not practical at any time for several causes like cost, time, required resources, and at the stage of preliminary design may be a number of building shapes take in to account. Building codes are generally able to account for the mean recurrence interval (MRI), the wind velocity, which is depends on the geographic location and the mean recurrence interval (MRI), roughness and topography and of the terrain that surrounding the building, directionality factor and wind speed and dynamic characteristics of the buildings.

Building codes are not able to account for building shape and shielding effects from adjacent buildings. Several studies have been carried out to compare how codes differ in treating wind loads on structures.

It should be noted that it is difficult to validate the actual wind loads a structure experiences. It is possible to obtain actual building cladding pressures due to wind but the most common way of validation is by comparing measured response (from a wind tunnel, or in situ testing) with predicted response. The empirical equations for wind pressure estimation on the buildings, comes from wind tunnel tests. So that it is better to take measurement from the field for validation purpose.

2.3.2 Wind Tunnel Test

In wind tunnel studies, scaled models of structures are subjected to scaled atmospheric wind in a controlled laboratory set-up. Then sensors installed on the model can measure the physical quantities of interest such as shear, moment, pressure etc. Later in the analysis, these model scale quantities are converted to prototype using model scale laws. Most of the complex architectural and structural innovations are being confirmed through wind tunnel tests. Wind tunnel tests are being done for almost all buildings above approximately 100 m. Even low buildings are being tested in some places like Miami, Florida where severe wind conditions persist.

Typical model scales are in the range of 1:300 ~ 1:500. Since the response of the structure is significantly influenced by its geometry, utmost care has to be taken in modeling the exact shape of the structure including all the external architectural ornaments such as fins, balconies etc. Typically, all elements more than 1ft can get modeled with the typical scale range noted above. However, certain simplification of

the external architectural features is allowed at the modeling stage by wind tunnel experts.

2.3.2.1 High Frequency Force Balance (HFFB)

The alternative method for aero elastic wind tunnel test is high-frequency force balance method when the priority for cost reduction and time saving instead of getting comprehensive information. In this method, the building model is created in appropriate scale with a rigid frame and putting on a high sensitive stiff force balance for measuring the overturning moment at the base of the building. After that analytically the acceleration, moment, shear, and dynamic displacement for the building at any height are determined.

2.3.2.2 High Frequency Pressure Integration (HFPI)

Measuring the pressure on the surface of the building in several locations simultaneously called the High Frequency Pressure Integration HFPI. The pressure taps must be installed on the building surface at a fine resolution, while the accurate data is required so as to get the same result as in case of using HFFB test.

Generally HFPI approach is more labor-intensive with respect to the determination of tap tributary areas, moment and torsion arms, as well as the physical installation of the pressure taps. Again, advances in graphics and modeling technology continue to help this process.

There remain some physical constraints with conducting HFPI studies. Slender structures provided limited space in which to run the instrumentation from the building face and out to the data acquisition system. In HFPI method inertial loads and wind-induced accelerations are estimated analytically Similar to HFFB test.

2.3.2.3 Aero-elastic Model Studies

In aero elastic studies, the building mass, stiffness and damping will be appropriately modeled. Typically, a central metal spine system is selected to represent the scaled down stiffness of the building in case of sway dominance. More complicated frame spine system is warranted in case torsional stiffness needs to be simulated. The outer shell connected to the spine represents the geometry of the building. Spine and shell together represent the scaled mass of the building. The damping is induced through simple magnetic or viscous damper. In aero elastic test, strain gauges fixed at the spine system at various heights are typically used to measure loads. These measured loads represent total loads including the resonant component. There is no need of estimating resonant loads analytically like in rigid model tests. Over and above, accelerations can be measured directly using accelerometers or lasers. Note that aero elastic models can move in air, so these moving models can interact with air and any change in force due to the movement of the model relative to the wind flow will be captured in measurements. These motion-dependent or 'aero elastic' forces are not experienced by rigid stationary models used in HFPI or HFFB tests.

However, aero elastic forces seem to be minimal and need not be considered for design in majority of the building cases. Typical buildings are not too tall and slender and they are massive as well, where aero elastic effects are negligible. In such cases, less expensive HFFB and HFPI tests can be utilized to obtain wind-induced response for design. When the building become too slender of the order of $h/b > 10$, or too tall above 500 m or too light and tapered with steel as the medium, then one would have to consider aero elastic tests if there is enough information warrant the test after a simple desktop study or HFFB/HFPI initial test.

2.3.3 Computational Fluid Dynamics (CFD)

Computational fluid dynamics (CFD) to analyze and solve problems that involve fluid flows, change several sets of physical laws such as conservation of mass, conservation of energy, conservation of momentum, etc. from a differential equation form to an algebraic equation, which is called numerical method. There are a number of numerical solution methods to solve the fluid flow problems like finite difference method, finite element method, and finite volume method. Most of the commercial (CFD) codes using finite volume methods as implemented in the (ANSYS FLUENT) code.

The CFD analysis composed of three stages; the pre-processor, the solver, and the Post-processor. Preprocessor is defined as a program that processes input data to produce output that is used as an input to the processor. The solver discretizes the differential equations converting them to algebraic equations that can be solved numerically using the finite volume method. Finally the post-processor is a tool that allows the interpretation of the solution in the form of graphs, plots, charts, and also can export the results to Microsoft Excel for making graphs and charts.

2.4 History of the Subject

Between 1931 and 1936, when the Empire State Building was constructed, J.Rathbun made full-scale measurements on it Rathbun (1940). Earlier in 1933, Dryden & Hill made measurements on a five-foot scaled model of the Empire State Building.

The wind sensitivity of buildings and structures depends on several factors, the most important of which are the meteorological properties of the wind, type of exposure, and the aerodynamic and mechanical characteristics of the structure, An inventory of those various factors is presented, including indications of their relative influence on

the global response Davenport (1998).

Holmes discusses the progress made in understanding wind loads on structures, and related aspects of wind engineering, emerging issues in 2003, and prospects for the next forty years. Although the name wind engineering was coined in the nineteen - seventies, resulting in the International Conference on 'Wind Effects on Buildings and Structures' becoming the International Conference on 'Wind Engineering' in 1979, the foundations of modern wind engineering were firmly set in the early nineteen -sixties. Several papers in the 1st International Conference on Wind Effects on Buildings and Structures at Teddington, U.K. in 1963 set the scene for the next forty years Holmes (2003).

2.4.1 Dynamic Analysis of Wind Force

Whitbread (1963) has presented an account of various flow parameters required to be matched in the wind tunnels and concluded that Jensen's (1958) model law provided satisfactory answers using floor roughening devices.

(Davenport and Isyumov 1967) have discussed various available techniques to simulate the Atmospheric Boundary Layer (ABL) in the long test section wind tunnels. They have emphasized that for correct modeling of flow complete turbulence characteristics including velocity profile, turbulence intensity profile, length scales and energy spectrum should be made available for natural wind. Flow characteristics in the new boundary layer wind tunnel at the University of Western Ontario are presented. 'Power law' variation of velocity profile is used. Counihan (1969) evaluated the use of a system of 'elliptic wedge' generators and a castellated barrier to produce a simulated rough wall boundary layer. Good agreement between the boundary layer flow so produced and neutral atmospheric boundary layer is

obtained.

(Fujimoto et al. 1975) have tested a 1:400 scaled aero elastic model of rectangular tall building (1:1.2:3.75) in smooth flow and two boundary layer flows. Values of along wind and across wind response are presented versus reduced velocity and a relationship is established. Experimental gust factors are compared with Davenport (1967). A four 10 mass model was also tested in natural wind, and contribution of higher modes is reported to be negligible on displacements and about 10% on accelerations.

Cermak (1977) states that a common procedure is to mount the model on a set of gimbals fixed to a rigid platform placed beneath the wind tunnel floor. Two pairs of mutually perpendicular helical springs attached to a rod rigidly fixed to the structural shell and passing below the gimbals provide the desired natural frequencies. Strain - gauges attached to the spring mounts can be used to give a voltage output proportional to sway amplitude. Adjustable magnetic damping is provided conveniently by attaching to the support rod a metal plate that passes between the poles of an electromagnet. Variation of current through the magnet permits control of critical damping ratio.

Parera (1978) studied the interaction between along wind and across wind vibrations of tall slender structures (1:1:6.3) using one degree -of-freedom and two degree-of-freedom aero elastic models. A new gimbal system to allow either one degree of freedom (D.O.F) or two degree of freedom (D.O.F) is also developed.

Cermak contributed significantly towards the laboratory simulation of atmospheric boundary layer ABL, between 1960 and 1990. His works (Cermak, 1977, 1979, 1981, 1982, 1984, 1987 and 1990) have treated various aspects of ABL

characteristics and simulation in detail. Wind tunnel design criteria have been established. Mathematical similarity criterion has been discussed and governing equations have been formulated. Uses of short test section wind tunnels with vortex generators and grids have been outlined. Closed-circuit meteorological wind tunnels have been designed with flexible ceilings and temperature control facility.

(Katagiri et al., 1995) have described a new type of multi degree -of-freedom aero elastic model. Experimental results of multi degree of freedom (M.D.O.F) model are compared with dynamic force balance tests and two degree of freedom aero elastic model tests and a good agreement is seen.

(Nakayama et al., 1995) presented their study on a super tall building with tapered cross -section. In first part the study is aimed at comparing the various wind tunnel modeling techniques. In the second part results of unsteady aerodynamic forces measured using manifold pressure taps at nine levels are presented. Also effects of edge configurations and tapering are studied.

(Holmes et al., 2003) discusses mode shape corrections and reviews processing methodologies for the determination of the overall wind loading and response of tall buildings using the high-frequency base balance technique. It is concluded that mode shape correction factors currently used for twist modes, are conservative. The effect of cross-correlations between base moments is found to be significant when calculating the response for coupled modes.

In the present paper, (Lin et al. 2005) local wind forces on tall buildings are investigated in terms of mean and RMS force coefficients, power spectral density, and span wise correlation and coherence. The effects of three parameters, elevation" aspect ratio, and side ratio, on bluff body flow and thereby on the local wind forces

are discussed. The overall loads and base moments are obtained by integration of local wind forces. Comparisons are made with results obtained from high-frequency force balances in two wind tunnels. Simulation of atmospheric boundary layer inside the test section of the open type wind tunnel at the Department of Civil Engineering, Ruhr University, and Bochum, Germany is attempted. Trapezoidal spires or castellated tripping fence are used for horizontal vortex generation, while the elliptical shark fins are used for vertical vortex generation. Square grids are also used to increase the level of turbulence in flow. Velocity data are obtained in two directions using two cross-wire hot wire probes of Dantec Dynamics make at different heights from the test section floor. The mean wind speed, RMS wind speed and integral length scale are obtained at different heights. These values are compared with corresponding field data obtainable from Engineering Science Data Unit (ESDU) assuming different geometric scales by (Mitra and Kasperski 2006). The analysis shows that with a geometric scale ratio of 1:200 to 1:150, the simulated boundary layer can be considered as the simulation of open country boundary layer up to a level of 30 to 35 meters in full scale.

Unusual structural shapes arising out of daring architectural forms need wind tunnel studies to assess the wind forces on such structures. Paper presents the results of a wind tunnel model testing of a 60 m high war memorial at Jammu. The test results are particularly useful in the design of the shield and its attachments with the tower (Gairola et al., 2006).

(Steckley et al 1992) studied the procedure for determining wind pressures on the exterior cladding of tall buildings. The methods used in a pressure model study are reviewed including measurement system frequency response, the determination of peak pressure coefficients, combining wind tunnel and meteorological data and

evaluating internal pressures. In addition, an assessment is made of the uncertainties involved in wind tunnel testing as compared with using building code methods.

The design of tall building is often influenced by wind-induced vibration such as accelerations in the matter of occupants comfort. Consequently, vibration periods and damping becomes important parameter in the determination of such motions. This paper is concerned with the natural periods and damping ratios of steel buildings. It describes the vibration measurement methods employed for testing buildings and presents reliable methods of assessing natural period and damping from ambient vibration tests. This paper describes the findings from full -scale measurement of micro-tremor vibration of 21 typical high-rise buildings in Korea. Regression formulas of natural periods and damping ratios for steel -framed tall buildings are suggested. Finally, obtained natural periods arc compared with empirical expressions of structural standards and eigenvalue analysis Yoon (2003).

2.4.2 Analytical Work

Davenport (1963b) attempts to trace the involution of a satisfactory to the loading of structures by gusts. It is suggested that a statistical approach based on the concepts of the stationary random series appears to offer a promising solution. Some experiments to determine the aerodynamic response of structures to fluctuating turbulent flow are described. Example are given of the application statistical approach to estimate the wind loading on a variety of structures, in noting including long span cables, suspension bridge, towers and skyscrapers.

(Vellozzi and Cohen 1968) published a procedure for the along wind response of tall buildings in which a reduction factor was introduced for the fluctuating pressures on the leeward face of a building as it is understood that there is no perfect correlation

between fluctuating pressures on windward and leeward faces of a building. However, it was shown by Simiu (1973a) that owing to the manner in which this factor is applied, the procedure of Vellozzi & Cohen underestimates the resonant amplification effects.

On the basis of his analysis and experiments, Vickery developed a further refinement of the Gust Factor Method Vickery (1971), As Vickery notes, his method tended to give conservative results for aspect ratio over four. Vickery concluded that his refined method could predict a building gust factor to a typical accuracy of 5 -10% for well-defined basic data, compared with other methods. Vellozzi and Cohen (1968) published a procedure for the along wind response of tall buildings in which a reduction factor was introduced for the fluctuating pressures on the leeward face of a building as it is understood that there is no perfect correlation between fluctuating pressures on windward and leeward faces of a building.

It was shown by Simiu (1973a) that owing to the manner in which this factor is applied, the procedure of Vellozzi & Cohen underestimates the resonant amplification effects. (Simiu, 1973a, 1974b, 1976, 1980) has developed a procedure for determination of along wind response incorporating meteorological parameters. He showed that dynamic response of three dimensional tall structures may be represented as a sum of contributions due to the pressures on the windward side, the pressures on the leeward side, and the along wind cross-correlation of these pressures. Later, he presented improved forms of longitudinal wind spectra in which the variation of spectra with height is taken into account. A program for the computation of the along wind deflection and accelerations was developed incorporating these meteorological and aero dynamical changes (Simiu and Lozier 1975) which was further modified by Simiu in 1980. Graphs and charts have been

developed for the simplified hand calculations (Simiu, 1976) , 1980).

(Peyrot et al., 1974) presented a method in which Wind forces at discrete points on a tall building are simulated on the digital computer as a multi-dimensional stochastic process. The cross-correlation structure of the wind is treated in a simplified manner. Building responses to wind samples are obtained in the time domain by the finite element method. Mathematical models of both wind and building are designed to minimize computer times and yet retain the essential characteristics of the response. The random response of tall buildings to wind loading can be studied either in the frequency domain or in the time domain.

(Takeno et al., 1975) studied the effect of wind velocity fluctuations on a simple elastic structure consisting of a concentrated mass. The wind induced response of a continuous structure is due mainly to drag and lift forces oriented in the direction parallel and normal to the wind flow, respectively. Due to the spatial variation of mean and fluctuating wind velocities, these forces are function of time and space. The lift force is produced by alternating oscillation of vortices, while the main contribution to the drag force comes from the wake formed on the leeward side of the structure. At critical wind velocities there is also a possibility of self-excited oscillation known as galloping. (Yang and Lin, 1981) have used a transfer matrix approach for analyzing the wind induced vibrations of a multi-story building.

Contributions of (Yang and Lin, 1981), (Islam et al., 1990) and Kareem (1992) towards the estimation of dynamic response of tall rectangular buildings using random vibration theory/transfer matrix formulation, and pressure measurements on faces and evaluating the covariance integration have provided alternate analytical solutions of the problem.

Isyumov (1982) has discussed the use of 'direct' aero-elastic simulations for the study of dynamic behavior of prototypes. A review of the aero-elastic model requirements is presented. Isyumov has described a 'stick' type two degree -of-freedom model and also multi degree-of-freedom aero elastic models.

The problem of dynamic along wind response of structures to forces induced by atmospheric turbulence is treated in this paper Solari (1982). Starting from the classical formulation, the study analyzes the behavior of two structural standard models, called point-like and three dimensional, respectively. The treatment of the problem presented in the paper leads to a closed form expression of the along wind response. The remarkable simplicity and the very high precision of the proposed method is pointed out in general terms and illustrated by two examples. In conclusion some prospects for possible future applications referred to this solution are outlined and briefly discussed.

Reinhold (1983) describes use of aero elastic and elastic models for the study of wind effects. A new technique using numerous pressure transducers to directly measure the fluctuating wind loads is presented. He has suggested the use of pressure transducers with aero elastic models.

Solari (1987b) formulates a theoretical consistent definition of "wind response spectrum" according to which the structural behavior to wind gusts can be evaluated, with a high level of precision and simplicity, by both an approximate dynamic analysis and an equivalent static approach. The method herein presented is based upon the equivalent wind spectrum technique, by means of which wind is schematized as a stochastic stationary Gaussian process characterized by a mean velocity profile on which an equivalent turbulent fluctuation, perfectly coherent in

space, is superimposed.

Effects of orientation of principal axis of stiffness on the dynamic response of slender square building model have been reported by (Isyumov et al., 1990). 1:1:5 & 1:1:10 proportioned 'stick' type aero elastic models have been used. Orienting the square building's principal stiffness axis along the diagonals helps in reducing the response. Effect of frequency separation in two directions is also discussed.

(Xie et al., 1999) state, for a building design there are usually three wind load components to consider: two orthogonal horizontal loads; and one torsional load. As each load component generally does not reach its maximum value at the same instant as the other components, nor even for the same wind direction, is it important to consider how these predicted peak load components should be combined for structural design.

(Chen et al., 2005) shows that High frequency force balance (HFFB) measurements have recently been utilized to identify the distribution of spatiotemporally varying fluctuating wind loads on buildings. These developments, predicated on their ability to compute any response component of interest, based on actual building characteristics, attempt to offer a framework that eliminates the need for mode shape corrections generally necessary in the traditional HFFB technique. To examine the effectiveness of these schemes with significant practical implications to wind tunnel modeling technology, this technical note utilizes a recent approach to identify the along wind loading on buildings. The predictions are compared to a widely utilized analytical loading model. It is noted that, akin to the traditional HFFB technique, the accuracy of these identification schemes clearly depends on the assumed wind loading model.

2.4.3 CFD simulation

The first attempt at turbulence modeling was made by Boussinesq (1877) who modeled turbulent flow simply by adding an eddy viscosity to the molecular viscosity. The idea behind is to take into account the enhanced momentum transport of the turbulent flow in the same way as molecular viscosity does for a laminar flow. Later Prandtl (1921) introduced the mixing-length concept that could be used to calculate a variable eddy viscosity, which led to the prediction of wall-bounded flows in fair agreement with experimental observation. In general, the eddy viscosity may be estimated as being proportional to the product of the velocity and length scales of the large energetic eddies. This concept has become the principle of the Eddy Viscosity Modeling (EVM), which is still the most widely-used model nowadays to represent the transport of flow turbulence in CFD studies.

Describing the movement of turbulent flows is, from a mathematical point of view, relatively straightforward as the motion of the fluid particles in space and time can be directly obtained from a governing set of differential equations. In the case of Newtonian fluids, which are isotropic and display linear relation between viscous stress tensor and rate-of-deformation tensor, the governing equations are the well-known Navier-Stokes equations. These equations, which reflect the conservation of continuity, momentum and energy in the flow, describe the evolution in time of the velocity and pressure fields of a moving fluid in a domain with specific boundary conditions under external force(s). Obtaining a realistic solution, however, is a challenging task. Numerical simulations, direct or simplified, are still facing several major difficulties in terms of computing time, accuracy and stability since the past memory as well as the future prediction is limited to short intervals of time only as the result of the nonlinear terms.

Despite the current setbacks, CFD has advanced to a certain degree of success in dealing with different types of fluid flows ranging from viscous to inviscid, laminar to turbulent and incompressible to highly compressible. Of various attempts to solve the governing equations, it is widely acknowledged that the direct numerical simulation (DNS) is too computationally expensive, and hence the general trend is to simplify the calculation process by averaging and modeling. Various models to generate flow turbulence have been developed, of which the most widely used are the k - ε models and the large eddy simulation (LES) models Murakami (1997). Simplifications for the k - ε models are made by introducing the modeled forms into k and ε transport equations (turbulence kinetic energy and its dissipation rate, respectively). The most popular k - ε models so far are the standard k - ε , renormalization group (RNG) k - ε and realizable k - ε models. In the case of LES, Navier - Stokes equations are filtered and large scales of motion are computed explicitly while the small or subgrid-scale motions are modeled. Proposed LES subgrid-scale models in the literature include the Smagorinsky – Lilly, dynamic Germano – Smagorinsky and Lagrangian dynamic mixed models Murakami (1997). Each of the mentioned models has certain advantages and disadvantages; in the case of k - ε models the computational effort is less but the turbulent energy is often over-estimated, while with LES the flow field can be predicted with higher accuracy but significant computational work is required. The choice of turbulence model therefore depends largely on a case-to-case basis, considering the particular flow condition as well as specific requirements of the outputs.

Computational wind engineering, being an applied field of the general CFD, emerged as a new area of research from the early 1990s. Since then, research has progressed significantly in the directions of both treating practical problems and finding new

applications. One of the major topics of interests is the study of wind flow around bluff bodies, which suggests a potential of conducting wind tunnel tests for tall buildings by supercomputer in particular. Pioneer works in this area include the studies in the 1970s and 1980s of numerical flows around two- and three-dimensional obstacles by (Hirt et. al., 1978), (Paterson and Apelt, 1986), and (Murakami and Mochida, 1988). In these works, flow simulation was attempted by solving the Navier-Stokes equations using finite difference techniques or the control volume method with either the standard k - ϵ or the standard Smagorinsky subgrid-scale turbulence model.

Since the 1990s there has been a rapid progression in the field of CFD with regard to the understanding and modeling of flow turbulence. New approaches as well as various modifications to the k - ϵ equations or the subgrid-scale modeling in LES have been proposed, the choices of turbulent model for numerical wind simulation hence were much widened. (Murakami and Mochida, 1995) used modified k - ϵ turbulence models developed by (Launder and Kato, 1993) and (Przulj and Younis, 1993) to generate 2D and 3D flows passing a square cylinder and compared the results with the LES solution. Similar experiments on a square cylinder were conducted by Lee (1997) in which conventional k - ϵ , RNG k - ϵ and low Reynolds number k - ϵ models were used for turbulence modeling instead. (Maruyama et al., 1999) used the dynamic subgrid-scale model proposed by (Germano et al., 1990) for LES computation of turbulent flow behind roughness elements. More recently, in the work of (Kataoka and Mizuno, 2002), artificial compressibility method was used for the computation of an incompressible flow passing 2D and 3D square cylinders.

Following the success of CFD in simulating turbulent flows over bluff bodies, a number of researches have attempted to evaluate the wind effects on buildings using

computational approach. (Murakami and Mochida, 1989) used the standard $k-\epsilon$ model to generate a numerical wind flow around a rectangular building and studied the flow field characteristics. Similarly, (Baskaran and Stathopoulos, 1993) conducted numerical tests on another building model and compared the resulted pressure coefficients with actual data. (Song and He, 1993) used LES instead to study the time-averaged velocity field and pressure distribution on a tall building in a weakly compressible flow. LES was also used by Selvam (1997) to predict the wind pressures field on the surfaces of the Texas Tech University building. (Swaddiwudhipong and Khan, 2002) recently investigated the wind load response of a 2D square building using LES. The results reported in these studies support the same idea that numerical wind tunnel tests of tall buildings, though still needs to be further refined and developed along with the capacity of the computing facilities, are definitely a viable alternative to the physical wind tunnel testing.

(Kumar A. et al., 2006) deals with the development of a numerical code to study flow over prismatic buildings in tandem arrangement by means of Large Eddy Simulations (LES). Flow over two buildings in succession with different spacing and heights have been considered in this study. Two dimensional unsteady Navier-Stokes equations have been solved using LES turbulence model. Streamline plots, isovorticity lines, surface pressure distribution (C_p) and velocity profiles have been obtained. Two and three dimensional experimental surface pressure distribution have been generated by conducting experiment in the 60cm×60cm test section wind tunnel facility available in the department and compared with predicted C_p values. Some significant differences have been observed between 2D and 3D surface pressure distributions.

CHAPTER 3

METHODOLOGY

3.1 Introduction

This chapter contains the definition of turbulence and modelling by k- ϵ model at the beginning. Then procedure of modeling and simulation of the domain from pre-processing to the post-processing stage described. Firstly, the assumptions to input data to the software were described. The simple analytical method used to validate the model. Good modeling qualification is important to get the correct selection in all simulations, in order to reduce the complexity of the problem and retaining the important characteristics. Identification and formulation of the flow problem in terms of computational domain, the physical and chemical properties of flow are necessary to be considered. Proper operation is made and suitable results were obtained from the CFD simulations.

3.2 Turbulence

Turbulence is an irregular motion, which, in general makes its appearance in fluids, gaseous or liquid, when they flow past solid surfaces, neighboring streams of the same fluid flow with different velocities or over one another. Turbulence is a flow characteristic in which the viscous forces are small compared to the inertial forces. In turbulent flow the viscous force has no ability to damp out small perturbations in boundary and initial condition. Instead, these perturbations are amplified causing rapid variation in pressure and velocity in space and time.

The criterion to determine the dominating force (inertial or viscous) is the Reynolds number

$$R_e = \frac{\rho V L}{\mu} \quad (3.1)$$

Where ρ is the density of the fluid, V is the velocity of flow, μ is the dynamic viscosity of the fluid and L is the characteristic length.

Turbulent flows occur over a large range of length and time scales, they are fully three-dimensional and time-dependent. Turbulent flows are much more irregular and intermittent in contrast with laminar flow. Turbulence typically develops as instability of laminar flow. For a real (i.e. viscous) fluid, these instabilities result from the interactions of the non-linear inertial terms and the viscous terms contained in the Navier-Stokes equations, which are very complex due to the fact that turbulence is rotational, three-dimensional and time-dependent.

The rotational and three-dimensional natures of turbulence are closely linked, as vortex stretching is required to maintain the constantly fluctuating vorticity. Since vortex stretching is absent in two-dimensional flows, turbulence must be three-dimensional. This implies that there are no two-dimensional approximations, thus making the issue of resolving turbulent flows a difficult problem.

The time-dependent nature of turbulence, with a wide range of time scales (i.e. frequencies), means that statistical averaging techniques are required to approximate random fluctuations. Time averaging, however, leads to correlations in the equations of motion that are unknown a priori. This is the classic closure problem of turbulence, which requires modeled expressions to account for the additional

unknowns, that is the primary focus of turbulence modeling.

Turbulence is a continuous phenomenon that exists on a large range of length and time scales, which are still larger than molecular scales. In order to visualize turbulent flows, one often refers to turbulent eddies, which can be thought of as a local swirling motion whose characteristic dimension is on the order of the local turbulence length scale. Turbulent eddies also overlap in space, where larger eddies carry smaller ones. As there exists a large range of different scales (or turbulent eddy sizes), an energy cascade exists by which energy is transferred from the larger scales to the smaller scales and eventually to the smallest scales where the energy is dissipated into heat energy by molecular viscosity. Turbulent flows are thus always dissipative.

Turbulent flows also exhibit a largely enhanced diffusivity. The turbulent diffusion greatly enhances the transfer of mass, momentum and energy. The apparent stresses, therefore, may be of several orders of magnitude greater than in the corresponding laminar case.

The fact, the Navier-Stokes equations are non-linear for turbulent flows that lead to interactions between fluctuations of different wavelengths and directions. The wavelengths of the motion may be as large as a characteristic scale on the order of the width of the flow, all the way to the smallest scales, which are limited by the viscous dissipation of energy. The action of vortex stretching is mainly responsible for spreading the motion over a wide range of wavelengths. Wavelengths, which are nearly comparable to the characteristic mean-flow scales, interact most strongly with the mean flow. This implies that the larger-scale turbulent eddies are most responsible for the energy transfer and enhanced diffusivity. In turn, these large

eddies cause random stretching of the vortex elements of the smaller eddies and energy cascades down from the largest to the smallest scales.

According to Newton's second law of motion for fluid flow, the continuity equation can be written as Taylor (2012);

$$\nabla \vec{V} = 0 \quad (3.2)$$

From continuity and the incompressible Navier-Stokes equations can be written in vector form as:

$$\Sigma \vec{F} = m \vec{a} \quad (3.3)$$

$$\rho \left(\frac{\partial \mathbf{v}}{\partial t} + \mathbf{v} \cdot \nabla \mathbf{v} \right) = -\nabla p + \nabla \cdot \mathbf{T} + \mathbf{f} \quad (3.4)$$

where \mathbf{v} is the flow velocity, ρ is the fluid density, p is the pressure, \mathbf{T} is the (deviatoric) component of the total stress tensor, which has the order two, and \mathbf{f} represents body forces (per unit volume) acting on the fluid and ∇ is the del operator. This is a statement of the conservation of momentum in a fluid and it is an application of Newton's second law to a continuum.

3.2.1 k- ϵ models

One of the most commonly used turbulence closure models is the k- ϵ model. The k- ϵ model is a two equation model that means it includes two extra transport equations to represent the turbulent properties of the flow. This allows a two equation model to account for history effects like convection and diffusion of turbulent energy. The k- ϵ model does not carry out well in the cases of large adverse pressure gradients. The first transported variable in the model is turbulent kinetic energy, k and the second transported variable is the dissipation rate of turbulent kinetic energy, ϵ .

Turbulence eddy dissipation is equal to the viscosity multiplied by the fluctuating vortices. An exact transport equation for the fluctuating vortices defined as the rate of dissipation of velocity fluctuations (Sarvan Mamaidi, 2009). The k - ε model is simple to implement and produce stable calculation and reasonable predictions for many flows. It is poor in predictions for swirling and rotating flows, flows with strong separation and axis symmetric jets. Well known k - ε models are; standard k - ε , realisable k - ε and re-normalising group (RNG) k - ε models. The realisable k - ε model was employed in the CFD simulations of this study.

3.2.1.1 The realizable k-epsilon model

The realizable k-epsilon model differs from the standard k-epsilon model in two important ways; the realizable k-epsilon model contains an alternative formulation for the turbulent viscosity and a modified transport equation for the dissipation rate, ε , has been derived from an exact equation for the transport of the mean-square vorticity fluctuation.

The term “realizable” means that the model satisfies certain mathematical constraints on the Reynolds stresses which are consistent with the physics of turbulent flows. Neither the standard k - ε nor the RNG k - ε models are realizable. Both the realizable and RNG k - ε models have shown substantial improvements over the standard k - ε model where the flow features include strong streamline curvature, vortices and rotation. Since the model is still relatively new, it is not clear in exactly which instances the realizable k - ε model consistently outperforms the RNG model. However, initial studies have shown that the realizable model provides the best performance of all the k - ε model versions for several validations of separated flows and flows with complex secondary flow features.

One of the weaknesses of the standard k - ε model lies with the modeled equation for the dissipation rate, ε . The poor prediction of the spreading rate for axisymmetric jets is considered to be mainly due to the modeled dissipation equation. The realizable k - ε model, proposed by Shih et al. (1995), was intended to address these deficiencies of k - ε models by adopting a new eddy-viscosity formula involving a variable C_μ which was originally proposed by Reynolds and a new model equation for dissipation rate, ε , based on the dynamic equation of the mean-square vorticity fluctuation.

One limitation of the realizable k - ε model is that it produces non-physical turbulent viscosities in situations when the computational domain contains both rotating and stationary fluid zones (e.g., multiple reference frames, rotating sliding meshes). This is due to the fact that the realizable k - ε model includes the effects of mean rotation in the definition of the turbulent viscosity. Consequently it is suitable for the present research; because of the work consist of one reference of frame without having any rotating sliding meshes.

3.3 Modeling and Simulation Procedure

In this part the modeling and the simulation procedures are described from pre-processing to solving and post-processing stages.

3.3.1 Pre-processing

It is the first and a very important part of the modeling. It contains the preliminary creation and generation of the model. The geometry is produced by using the Design Modular which is a part of the ANSYS workbench software as in the Figure 3.1. Then the mesh is generated on the pre-described geometry. Furthermore the physical and the chemical properties and the necessary boundary conditions are assigned to the software.

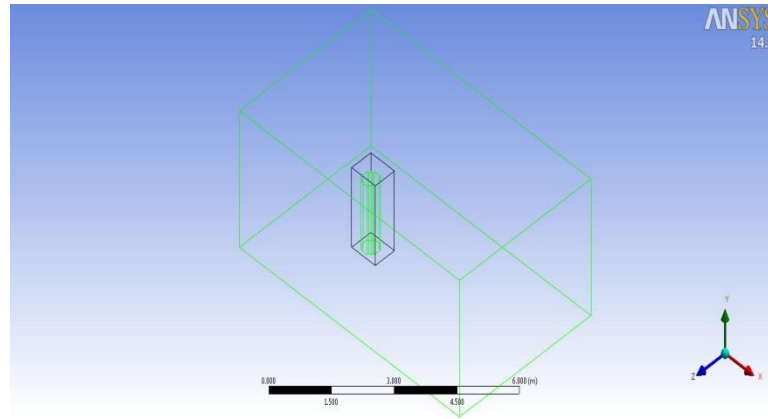


Figure 3.1 The whole domain of double recession building

3.3.1.1 Creating the model and defining the geometry

In Design Modeler the model of the building was created with a dimensional scale of 1:100. There are two steps for creating geometry regions. The first step is creating a model which represents the isolated building and the second step is creating the enclosure which represents the atmospheric boundary layer (ABL).

Three building models of different geometrical plans with equivalent areas of 1380 m² each one having a height of 183 m were tested. The first one has a rectangular plan area of 46*30 m (Table 3.1), the second has 46.5*30.5 m rectangular plan area with a single recession at four corners and the third one has 47.3*31.3 m rectangular plan area with a double recession at four corners, each recession was 3*3 m. The enclosure surrounding the model buildings, which signifies the virtual wind tunnel test, was 740*446*300 m (Table 3.2). The center of the model bases were placed at the 220 m far from the inlet, while in crosswise direction it was located at the center of the enclosure. The angle of the wind flow was set to be perpendicular to the width (46 m) of the models. Also the body of influence was created around the models in order to help refine the mesh sizes around the buildings. Figures 3.2, 3.3 and 3.4 represent the whole domain of double recession building in different point of views.

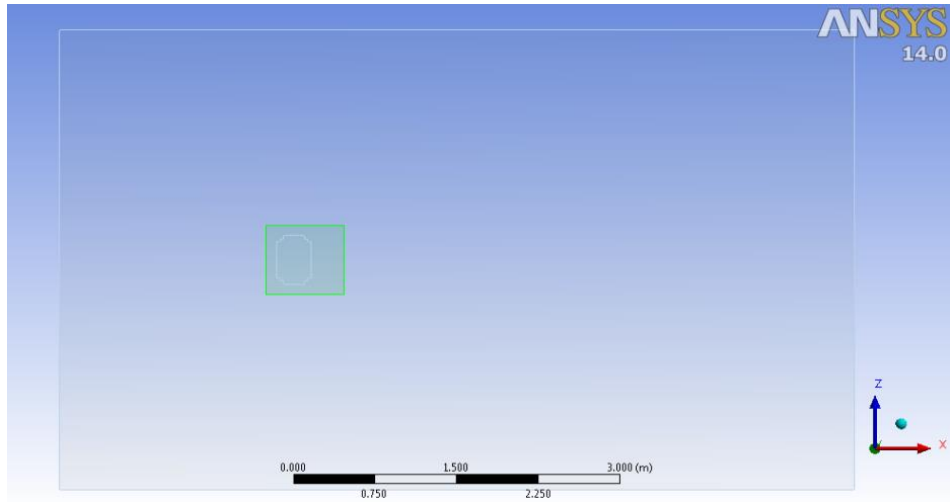


Figure 3.2 Top view of the domain of the double recession building model

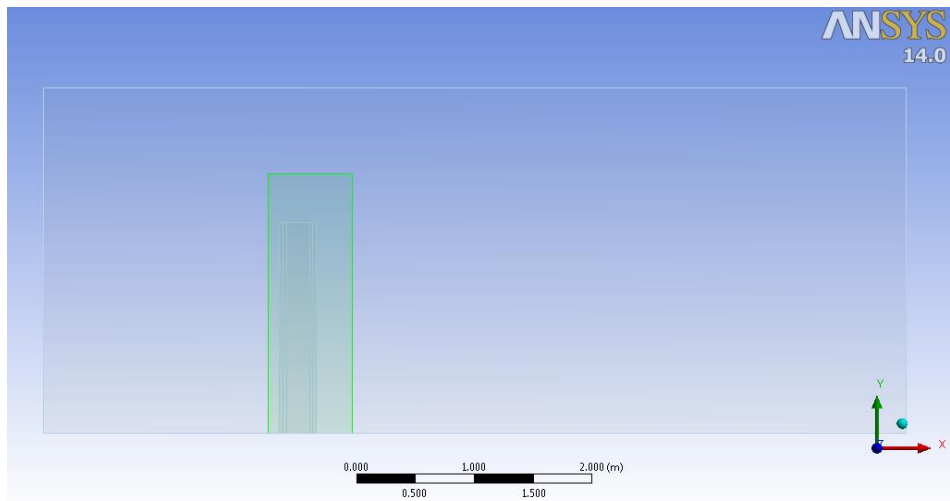


Figure 3.3 Side view of the domain of the double recession building model

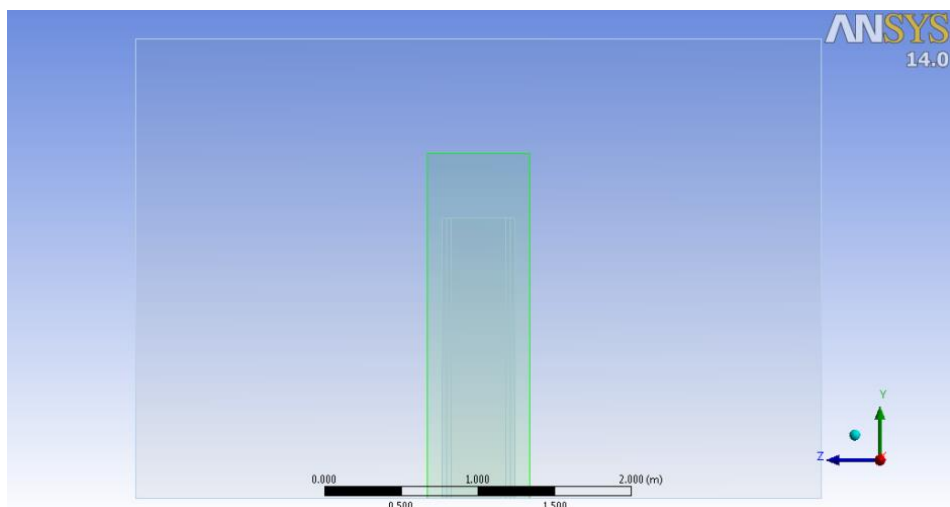


Figure 3.4 Front view of the domain of the double recession building model

Table 3.1 Dimensions of whole domain

Dimension	Length(m)
Length	740
Width	440
Height	300

Table 3.2 Dimensions of the three alternative building types

Description	rectangular	single recession	double recession
Width	46 m	46.5 m	47.3 m
Length	30 m	30.5 m	31.3 m
Height	183 m	183 m	183 m

3.3.1.2 Creating the boundary layer and meshing

When the model was created and defined, it should be discretized into a number of control volumes, which are called cells, for accuracy and control of the results. This operation is known as meshing. Figure 3.5 shows the meshing which has been performed on a model building. On the other hand, defining the boundary layers of the models, such as walls, surfaces, inlets, outlets and the building model and initial conditions are vital in CFD simulations.

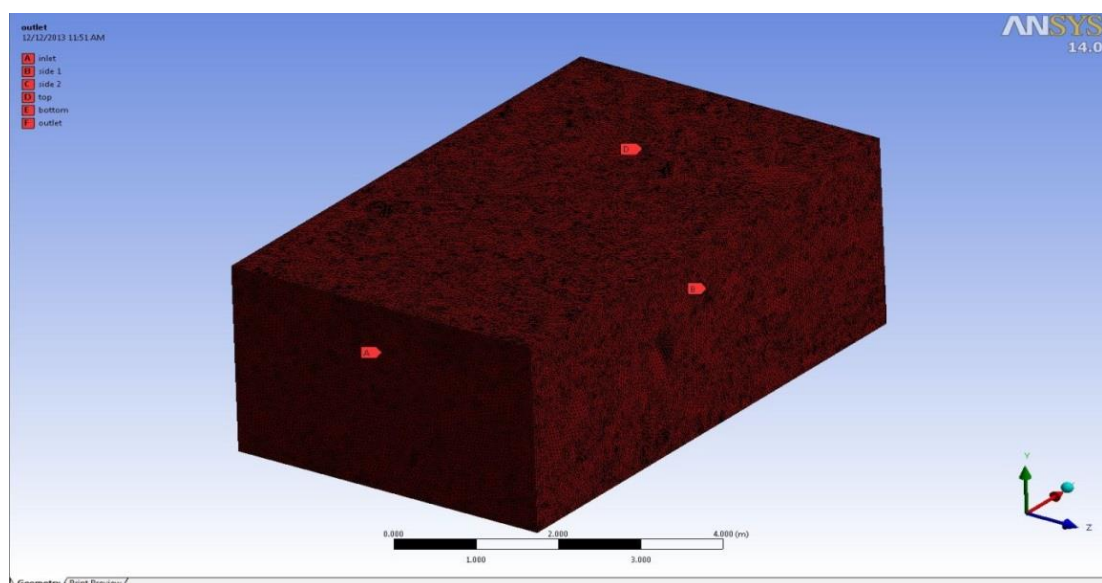


Figure 3.5 Meshing of the domain

To provide accurate results in regions close to the boundaries, where changes could be radical in flow characteristics, the mesh should be examined and refined especially on the building surfaces. In this study, the model in the double recession case was divided into 1,795,544 nodes and 10,434,775 elements. Figure 3.6 show the mesh metric of the building in double recession case model. Defining the boundary conditions is the final step of the meshing procedure. Each boundary condition in the model should be defined.

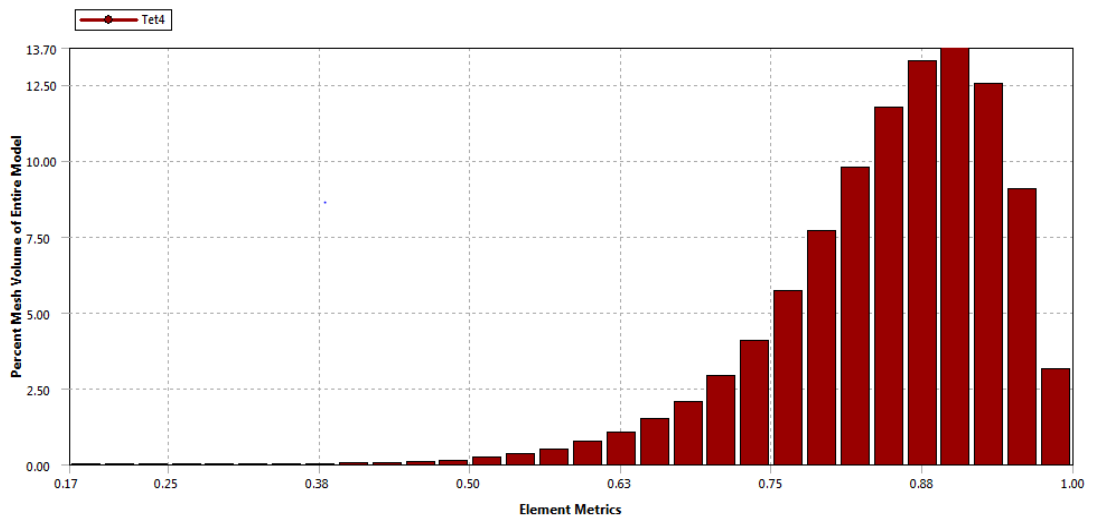


Figure 3.6 Mesh metric of the building in double recession model

In this model, the bed of the model is defined as bottom, sides are specified as the walls or symmetries, the top of the model is defined as surface, the entrance and exit of the air is defined as velocity inlet and velocity outlet respectively. Finally the building was specified. Before passing on to the setup process in the program, the mesh should be closed and updated. The different views of meshing rectangular building model are given in the Figures 3.7, 3.8, and 3.9.

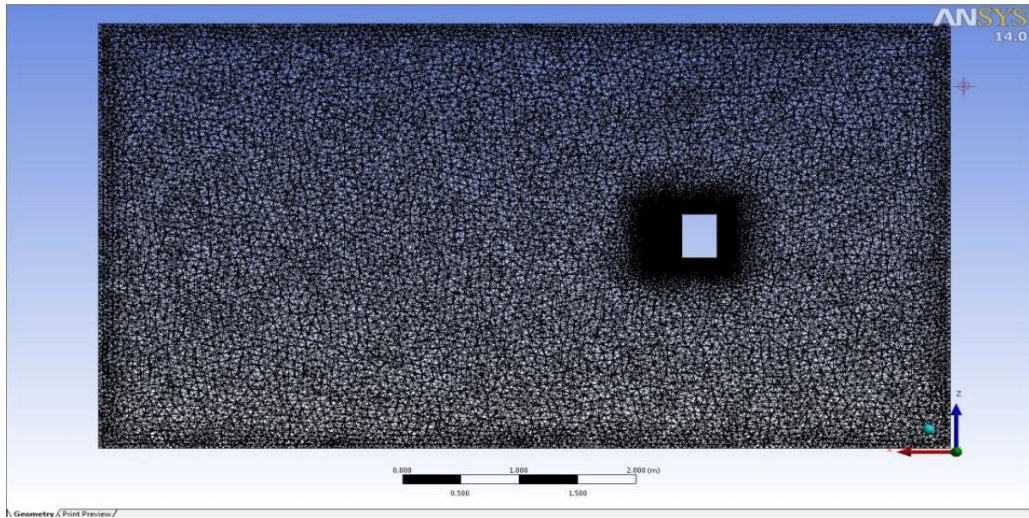


Figure 3.7 The top view of rectangular building model with the mesh

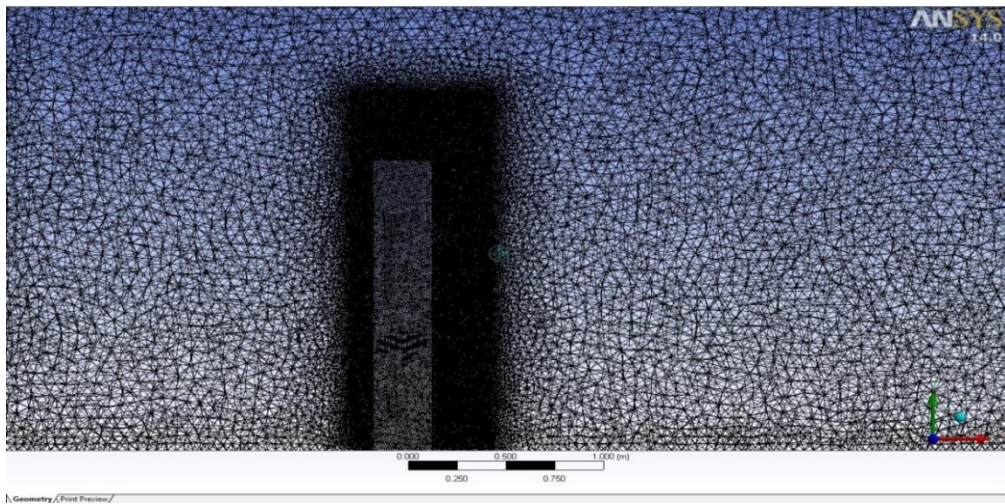


Figure 3.8 Side view of rectangular building model with the mesh

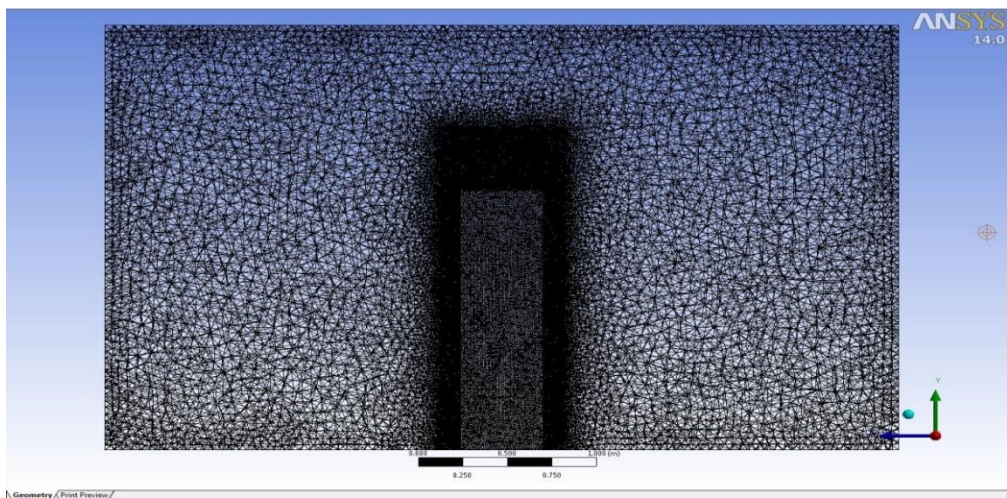


Figure 3.9 The vertical cross-section of rectangular building model with the mesh

3.3.2 Simulation

The generated mesh with boundary layers was integrated into the FLUENT which runs on ANSYS workbench software. Then the quality of the mesh was checked. Finally the physical phenomena and fluid properties were specified. The steps to simulate the model are defined in following parts.

3.3.2.1 The physical procedure

The solver take as pressure based type with absolute velocity formation for the 3D model. Then the multiphase model remain off, because of the fluid in this case is only air. Furthermore, $k-\varepsilon$ realizable (two equation) viscous closure model with standard wall functions was picked for the turbulent flow. All these properties are assumed to be constant over the model.

3.3.2.2 Defining the fluid properties

The fluid was selected as air and the necessary changes for viscosity, density, gravitational acceleration, etc. were performed. The fluid properties which were input to the software are given in Table 3.3.

Table 3.3 Properties of air

Property	Value
Density	1.225 kg/m ³
Viscosity	0.0000183 Pa.s
Temperature	20c

3.3.2.3 Specification of boundary conditions

In this stage, cell zone and boundary conditions were defined. The model has only one cell zone which is air. The inlet and the outlet boundary layers were selected as velocity inlet and pressure outlet respectively. The list of the boundary conditions is given in Table 3.4.

Table 3.4 The boundary conditions of the domain

Surface	Boundary type
Inlet	Velocity inlet
Outlet	Pressure outlet
Bottom	No slip wall
Top	Free slip wall
Right side	Free slip wall
Left side	Free slip wall

Due to the complex behavior of wind velocity profiles on different trains, the wind velocity profile at the inlet was input to the program by a user defined function (UDF), which was written in C++ and given in Appendix A.

3.3.3 Initialization and solution

In this step, the properties of the turbulence were defined and other factors were introduced. The inlet was taken as reference to initialize the solution. The active reference frame was chosen relative to the cell zone. The input velocity in the x-direction was introduced by inputting the user defined function (UDF) that represents variation of velocity with height, wind velocity was set to a value of 26 m/s at 2 m height from the ground and varied with height by power a coefficient of $\alpha = 0.15$ as it is shown in Appendix A. The number of iterations was fixed to 6 000 for a good conversion, the total required time for getting results was about 120 hours. The diagram which shows residuals vs. number of iterations for rectangular building model is given in Figure 3.10.

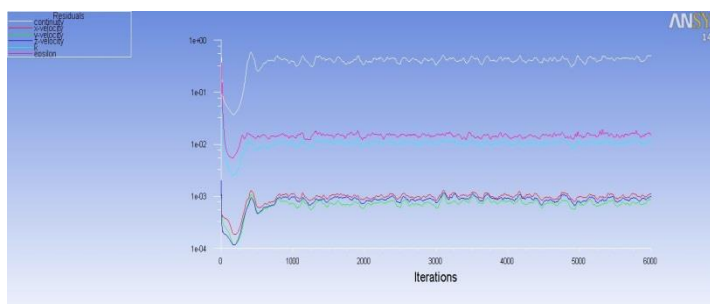


Figure 3.10 The residuals vs. number of iterations for rectangular building model

3.3.4 Post-processing

In the post-processing stage, the results can be screened and the flow characteristics such as; velocity, pressure can be plotted. The required representation style such as, vector or contour plot, surfaces and other visual preferences can be arranged. The post-processing results are given in Chapter 4.

CHAPTER 4

RESULTS AND DISCUSSIONS

This chapter provides the post-processing visualization and simulation results. The velocity and pressure on the building faces and in the whole domain, also other physical properties are presented. For validation purpose, the results obtained from the computational fluid dynamics (CFD) analyses were compared with a number of codes which determines wind effect on tall structures (Holmes et al. 2008).

4.1 Velocity profiles

Figures 4.1, 4.2, and 4.3, show the vertical velocity profiles along a line that passes through the center of the building and the whole domain for the building models with rectangular, single recession and double recession, respectively. It appears that in the inlet the wind velocity increases with increasing the height. The velocity profiles are taken at every 45 m interval at the upstream, where the last one is 20 m in the upstream of the building. Change in the velocity profiles due to the existence of the building is insignificant till 65 m upstream of the building. At the 20 m upstream of the building the velocity profiles start to deviate. The along wind velocity of the air flow increases in the regions over the height of the buildings, while it decreases below that height due to the structural obstacle, for all there building models.

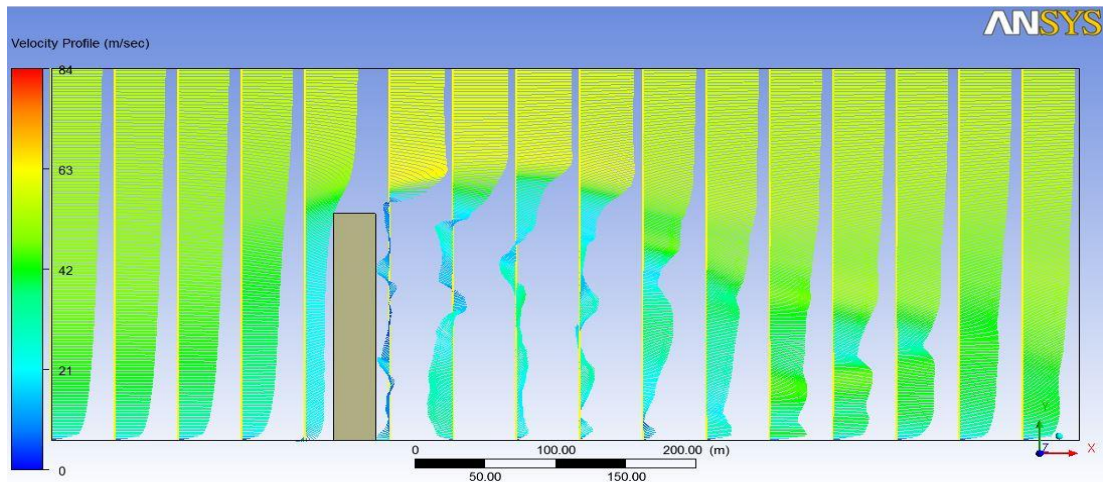


Figure 4.1 Vertical velocity profiles from the center of the rectangular building model

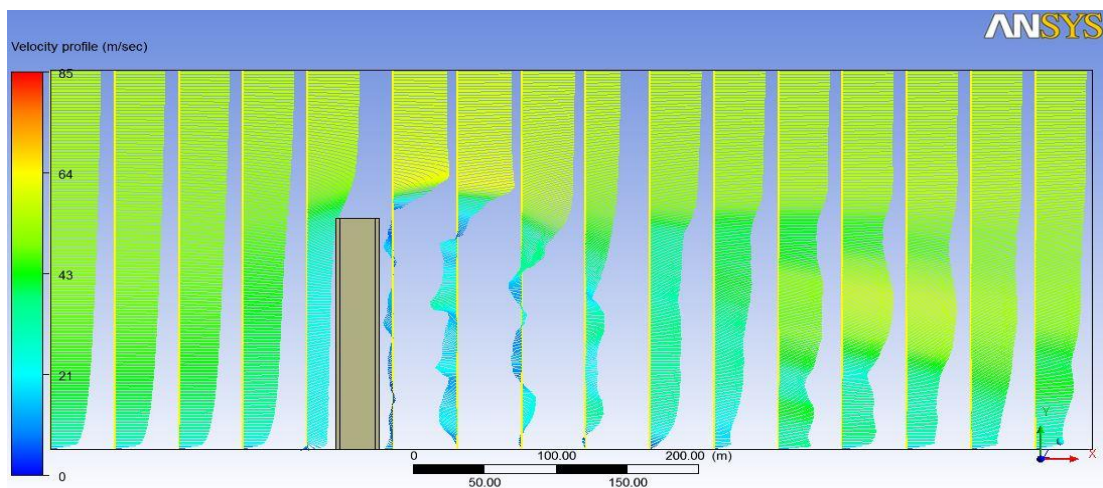


Figure 4.2 Vertical velocity profiles from the center of the single recession building model

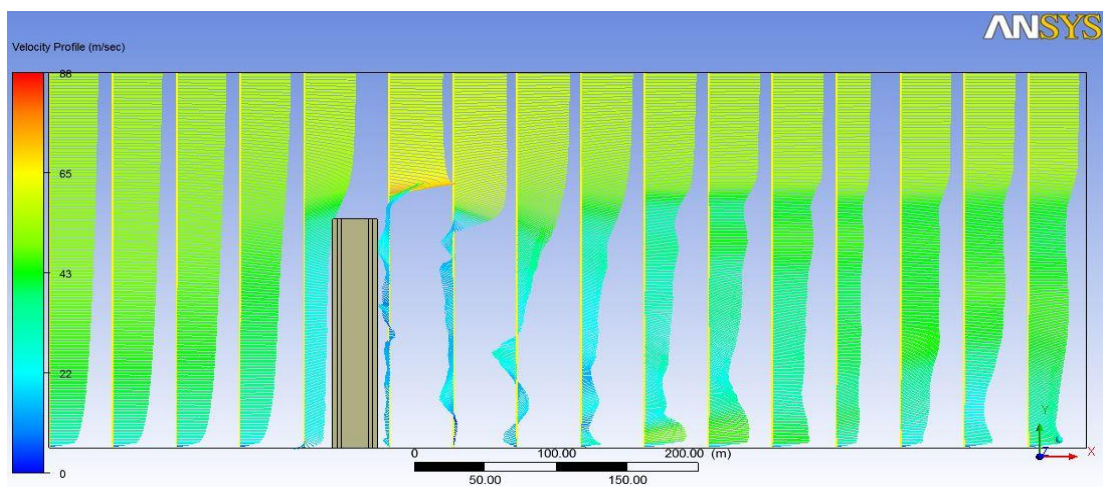


Figure 4.3 Vertical velocity profiles from the center of the double recession building model

4.2 Velocity streamlines

Streamlines are a family of imaginary curves which are tangent to the velocity vector of flow at any moment in time. They show instantaneously the direction a fluid element is expected to travel. In steady flows streamlines, pathlines and streaklines coincide. Figures 4.4 and 4.5 show the horizontal and the vertical streamlines for the double recession building model. At the inlet of the domain there is no turbulence in the flow and the streamlines are straight and parallel to one another. When the flow reaches to the building model, the turbulence takes place and flow becomes unsteady due to the resisting forces. Vortices are produced at the downstream of the building and the flow path remains unsteady as far as more than 500 m away from the model.

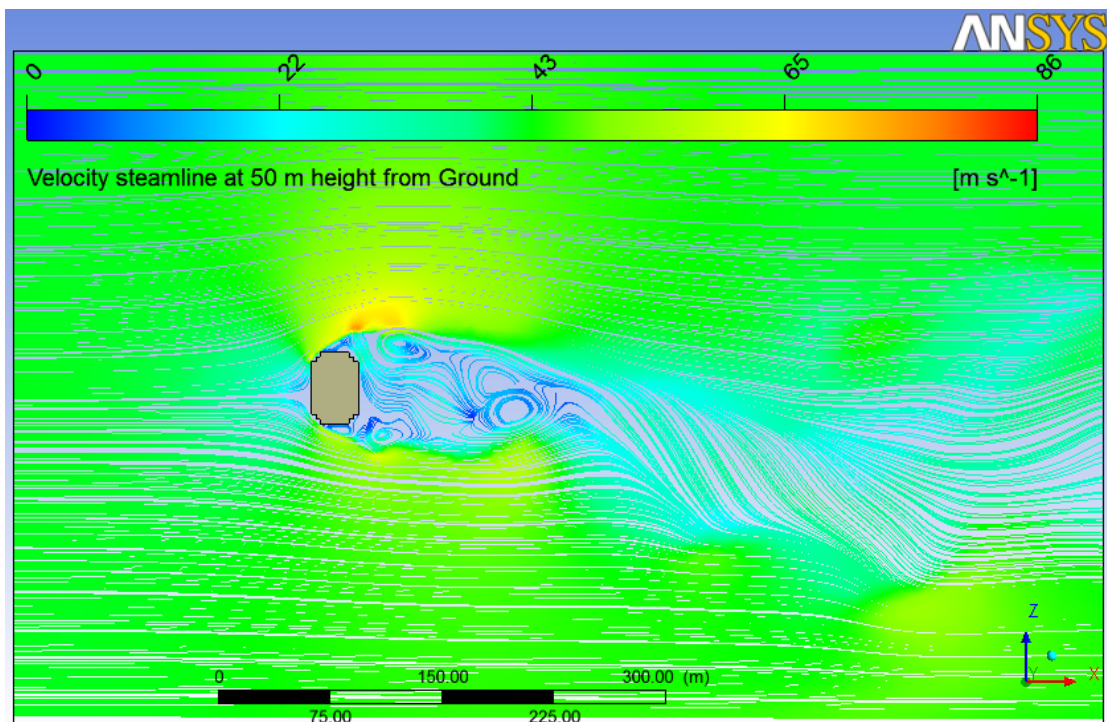


Figure 4.4 Horizontal velocity streamlines in the domain at height 50 m from ground for double recession building model

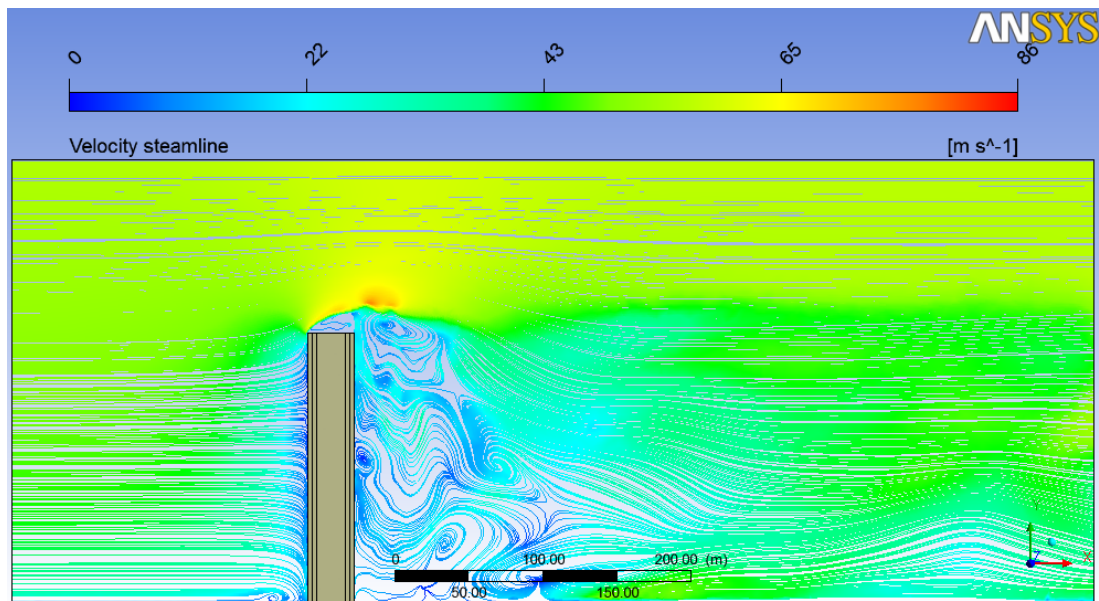


Figure 4.5 Vertical velocity streamlines in the domain at the center of the double recession building model

4.3 Velocity vectors

Figures 4.6, 4.7, 4.8, 4.9, 4.10 and 4.11 show the velocity vectors in the fluid domain where the flow around the building models are given in details. It is clear especially in the Figures 4.13, 4.15 and 4.17 that the energy dissipates due to flow re-circulation in the wake of the building models. The dissipation increases by corner recessions and makes diversion of the flow from the corners to the outward areas around the buildings. The point of stagnation is clearly observed in the center of the wind ward face of all three building models, where flow deviates to the left and the right sides of the buildings.

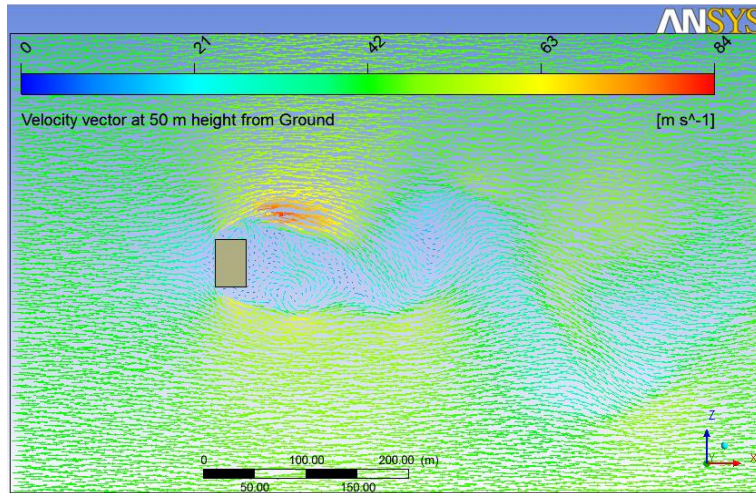


Figure 4.6 Horizontal velocity vectors for rectangular building at height of 50 m from the ground

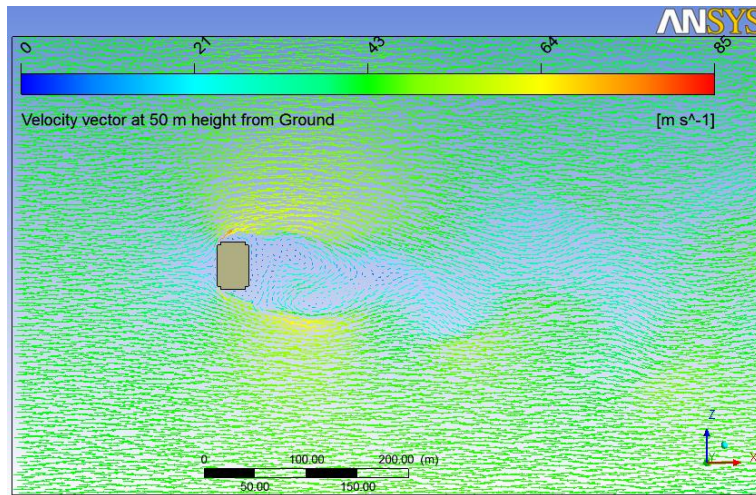


Figure 4.7 Horizontal velocity vectors for single recession at height of 50 m from the ground

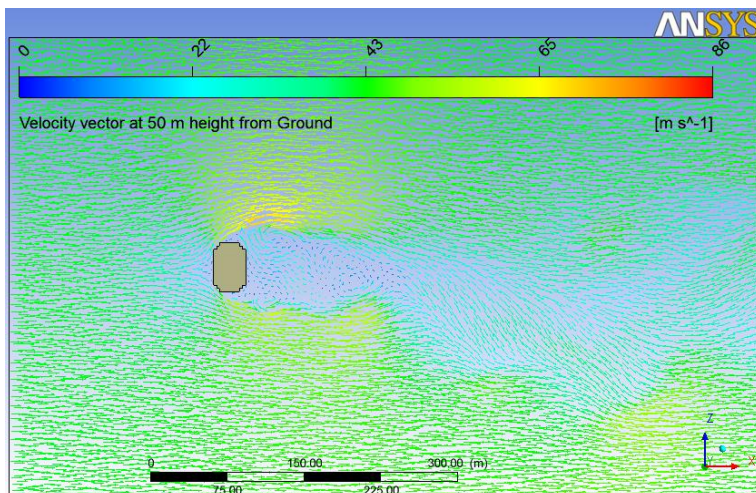


Figure 4.8 Horizontal velocity vectors in double recession building at height of 50 m from ground.

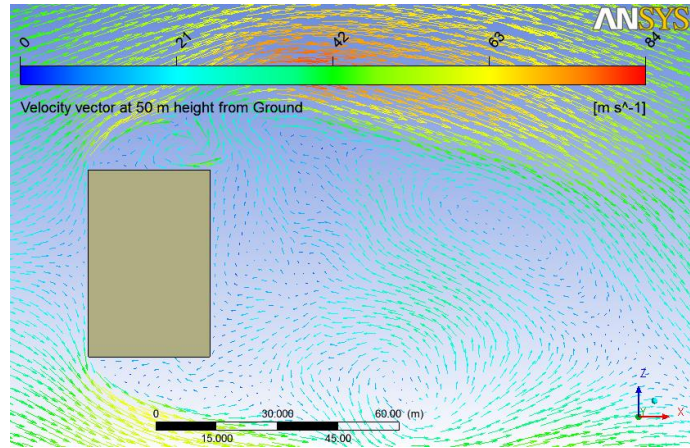


Figure 4.9 Horizontal velocity vectors for rectangular at height of 50 m from the ground near building

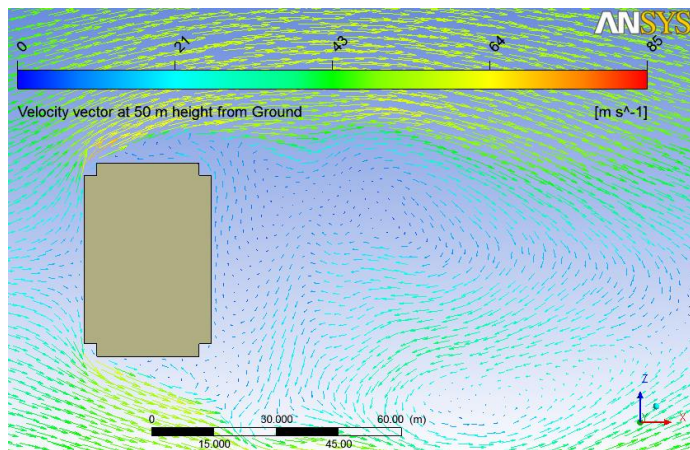


Figure 4.10 Horizontal velocity vectors for single recession at height of 50 m from the ground near building

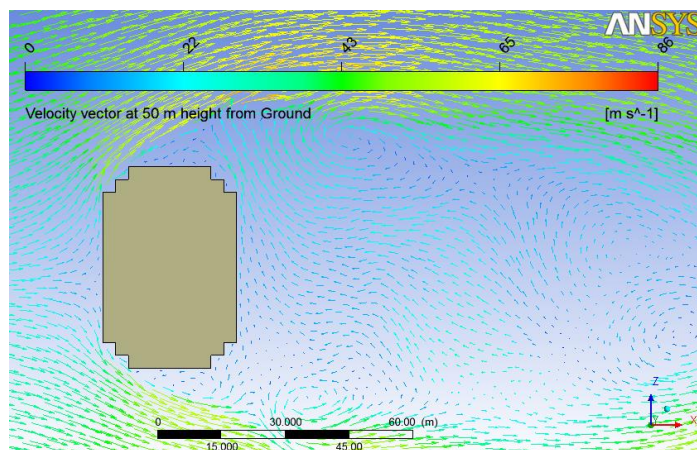


Figure 4.11 Horizontal velocity vectors for double recession at height of 50 m from the ground near building

4.4 Velocity contours

4.4.1 Horizontal velocity contour

As it is seen clearly in the Figures 4.12, 4.13 and 4.14, the velocity at the upstream of the building is not affected greatly by the building. When the flow reaches to the building the flow deforms to find the line of least resistance. The deformation takes place at the midway between the building and domain boundaries. At the downstream of the building the flow becomes turbulent. Using alternative building plan shapes does not appear to have a significant influence on the flow at the downstream of the building model and the whole domain.

4.4.2 Vertical velocity contours

The deformity of the vertical velocity distribution along the length of the domain has been studied as in the Figures 4.15, 4.16 and 4.17. The velocity is almost constant at the upstream in a specific height. The biggest decrease in the velocity occurs near the building. According to the Bernoulli's principle the pressure just upstream of the structure should be raised to its maximum value, since the velocity, thus the kinetic energy has its minimum value. This is the evidence of energy changing from one form to another.

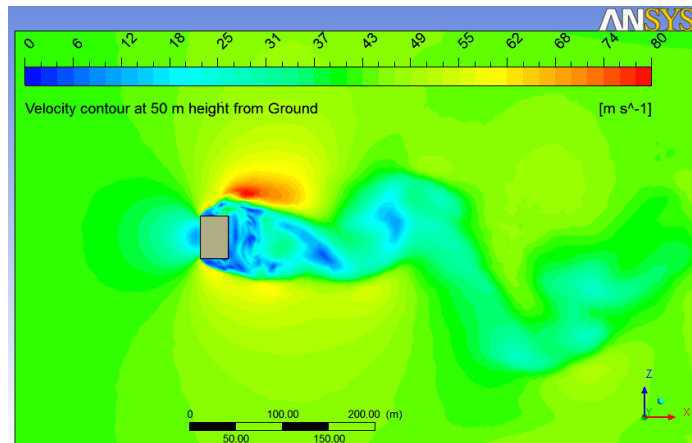


Figure 4.12 The velocity distribution at height of 50 m from ground for rectangular building

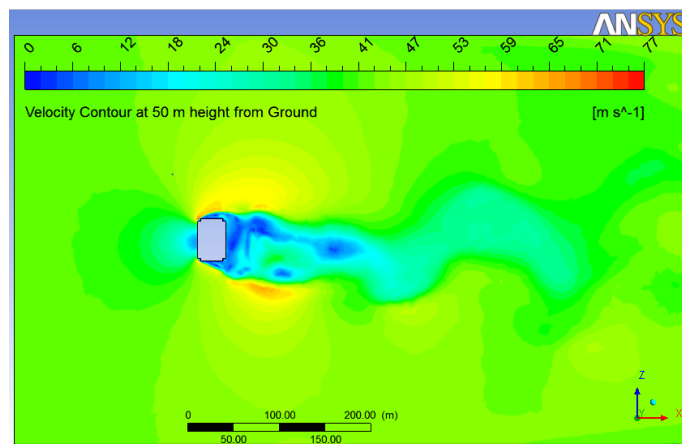


Figure 4.13 The velocity distribution at height of 50 m from ground for single recession building

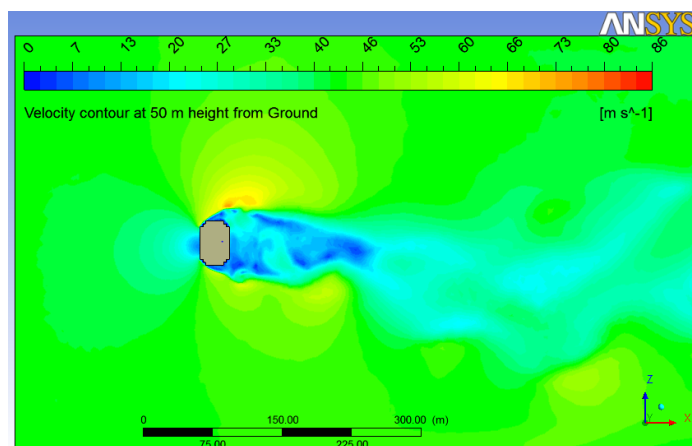


Figure 4.14 The velocity distribution at height of 50 m from ground for double recession building

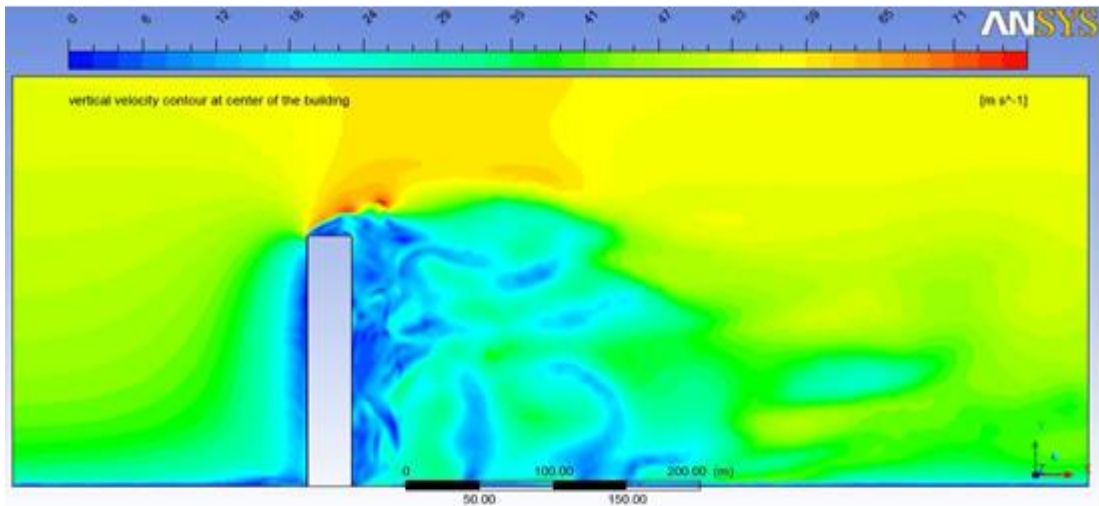


Figure 4.15 Vertical velocity contours from the center of rectangular building

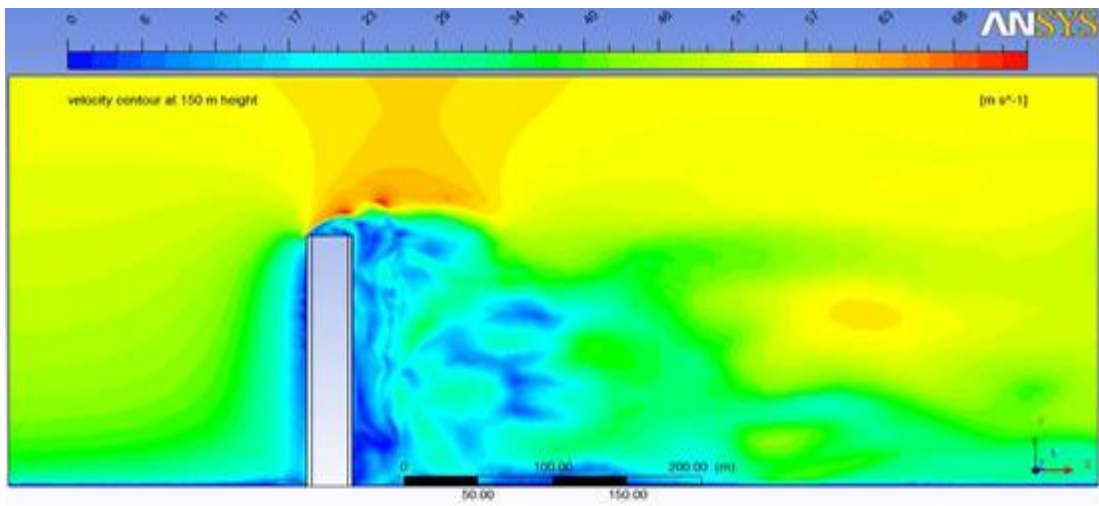


Figure 4.16 Vertical velocity contours from the center of single recession building

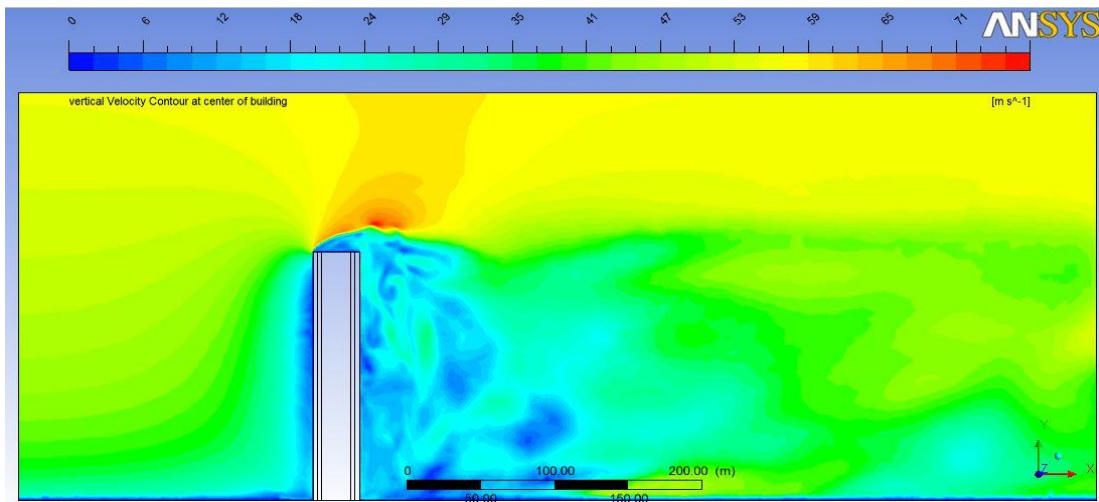


Figure 4.17 Vertical velocity contours from the center of double recession building

4.5 Pressure on the Building Faces

As it is seen in Figure 4.18, the along wind force on a building is composed of two components. The first component is the push force on the windward face, due to the positive pressure occurs at the upstream face of the structure. The second component is the suction force on the leeward face, attributable to the negative pressure created by vortex shedding which takes place in the wake of the building because of the recirculating flows and turbulence. The yellow color in Figure 4.15 represents the pushing force which is greater than 500 Pa and the green color characterizes suction force which is greater than 1200 Pa. It is obvious that the suction force is considered as the major force in the along wind and pushing as the minor force.

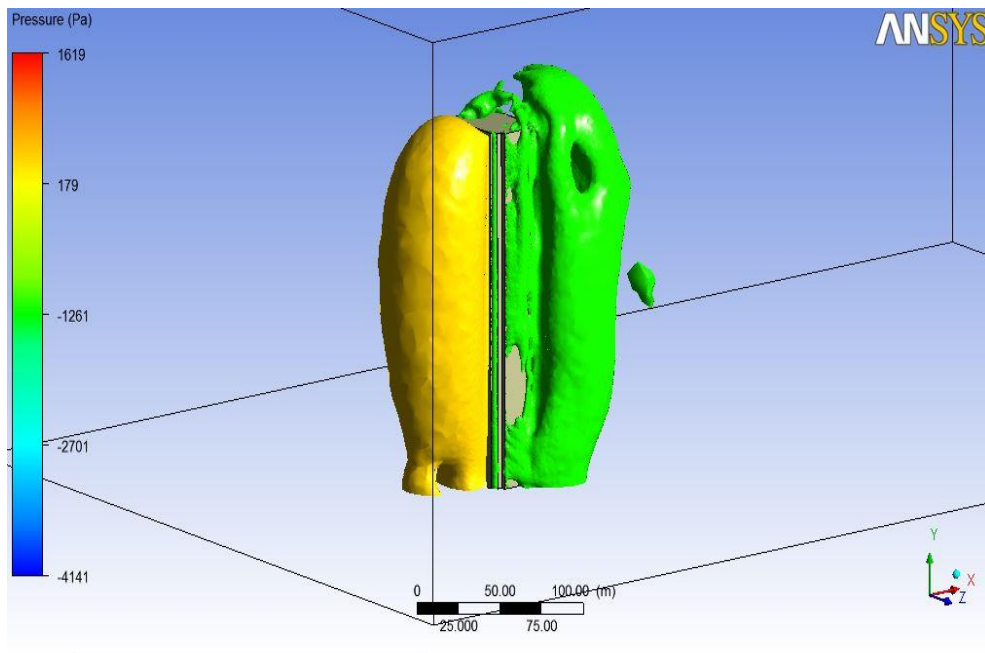


Figure 4.18 Pressure contour on windward and leeward faces of the double recession building

The pressure distribution over the windward and the leeward faces of the building models for all three cases studied here are illustrated in Figures 4.19 and 4.20, respectively. Generally the positive pressure increases with increasing of the height

from the ground, since the velocity magnitude is directly proportional to the elevation. While wind blows on the windward faces of the buildings, more quantity of kinetic form of energy converts into flow (pressure) energy at higher altitudes. In the rectangular building model, the forces due to positive pressure push the building on the entire windward face with a slight decrease at the edges. The decrease in the positive pressure at these edges is because of the change in the direction of wind. In the other two models the suction force in the recession areas has a great influence on reducing the total pushing force, especially in the single recession case. The corner recession in structures can be considered as an important parameter in decreasing the total windward force on the buildings faces. Suction forces, caused by the negative pressure, in the recession areas are sometimes twofold greater than the pushing force on the windward faces. This may cause discomfort in the balconies in such areas and even damage cladding of the structures. Variation of the pressure at the leeward faces of structures does not necessarily change with the height. However, recirculating wind flows and vortex shedding create an alternating negative pressure on the leeward face of the buildings, which leads to an alternating suction force on the surface of the structures.

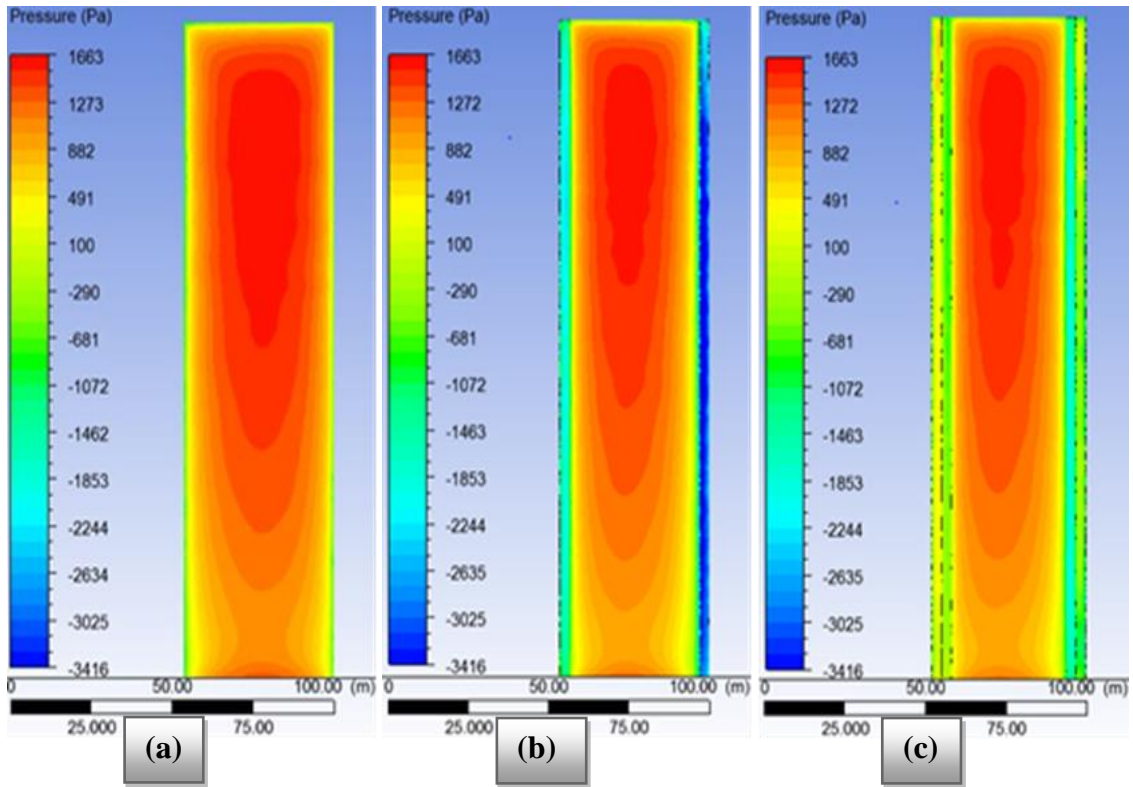


Figure 4.19 Pressure distribution on windward faces of all three building models
 (a)Rectangular (b) Single recession (c) Double recession

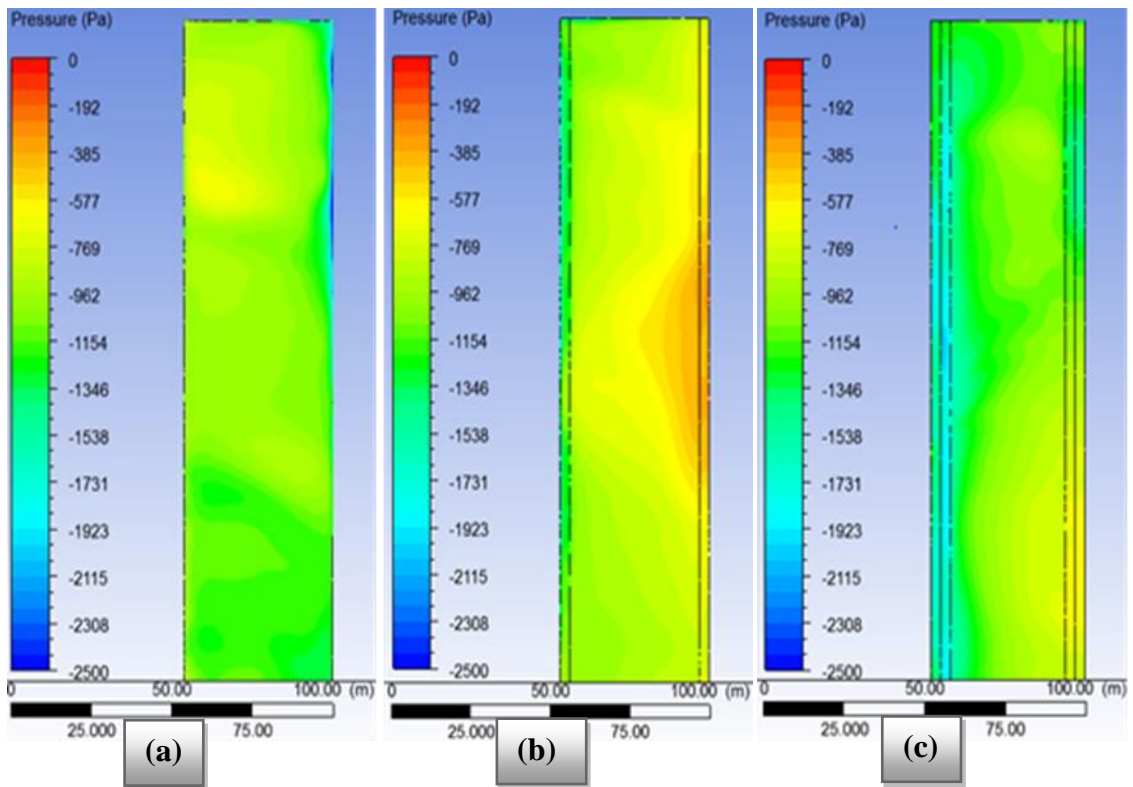


Figure 4.20 Pressure distribution on leeward faces of all three building models
 (a) Rectangular (b) Single recession (c) Double recession

4.6 Base Shear and Base Bending Moments

The pressure builds-up on the surfaces of tall structures generates a number of forces to be applied on high buildings. These horizontal forces cause a lateral reaction force to take place at the bottom of the structure, which is called base shear force or base shear. Base shear is an estimate of the maximum anticipated horizontal force that will take place as a result of seismic ground motion or dynamic wind forces at the base of a building. The horizontal wind loads also push the structure to be overtopped. The moment, which resists the overtopping of the building, is called the resisting moment or base bending moment. Figures 4.21 and 4.22 illustrate the along wind basic shear forces and basic bending moments calculated codes used in a number of countries around the world and the CFD simulation conducted in this study. It is clear from the charts, that there is an inordinate difference between the results of the codes and the CFD analyses, for both the along wind base shear and the bending moment. The CFD analyses have produced base shear and base moment results slightly greater than the average of the outcomes of the codes estimations. Furthermore, due to the forces applied on the crosswind surfaces of buildings and the alternating vortex shedding in the wake flow a lateral reaction force called base shear force and a base bending moment generate at the bottom of tall structures.

Figures 4.23 and 4.24 demonstrate the across wind basic shear forces and the basic bending moments calculated by several codes and the CFD simulation conducted in this investigation. The crosswind forces are considered as the major forces on tall structures when compared to windward forces (Gu et. al., 1999). Attributable to plan dimensions of the building models used in this study (Table 3.1), the across wind forces were calculated to be less than the along wind forces. The across wind base shear forces estimated by ANSYS FLUENT were found to be around 6.5% greater

than the average of the result calculated by the widely used codes. For base bending moment this difference has risen to 8.8%.

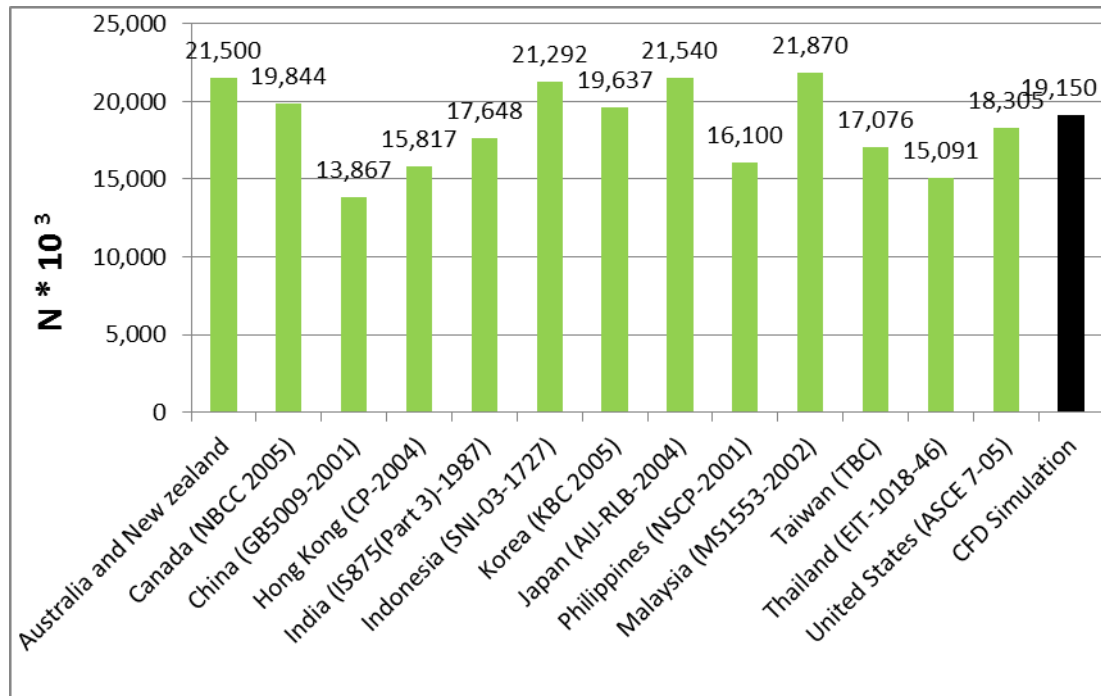


Figure 4.21 Base shear in the along wind direction by different codes and CFD Simulation

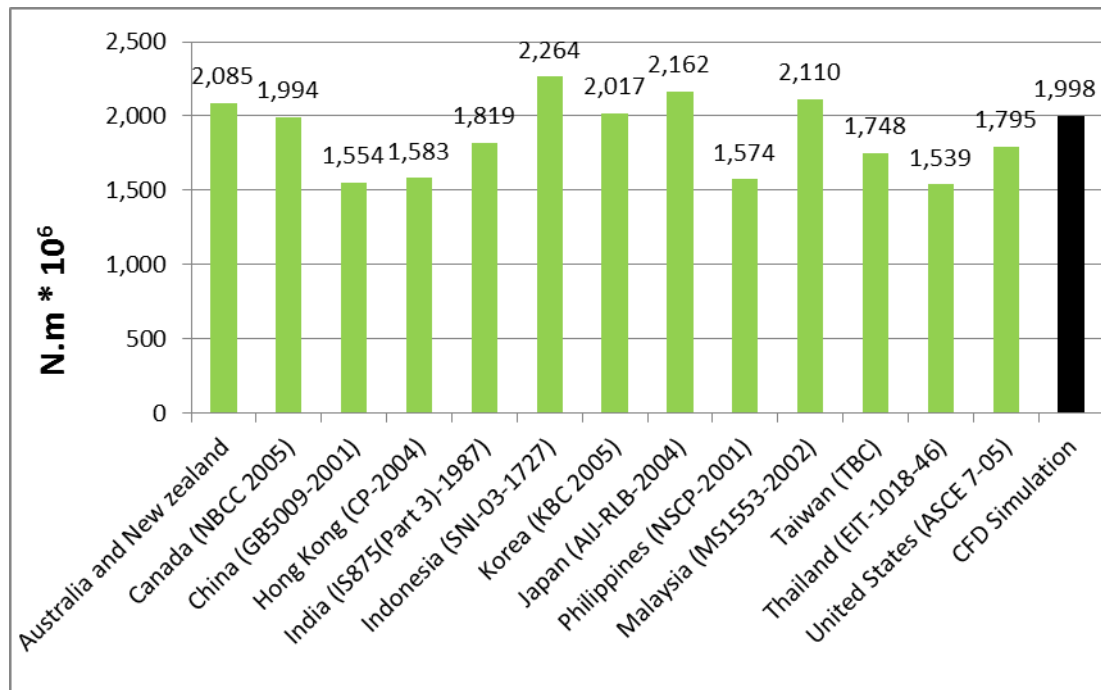


Figure 4.22 Base bending moment in the along wind direction by different codes and CFD Simulation

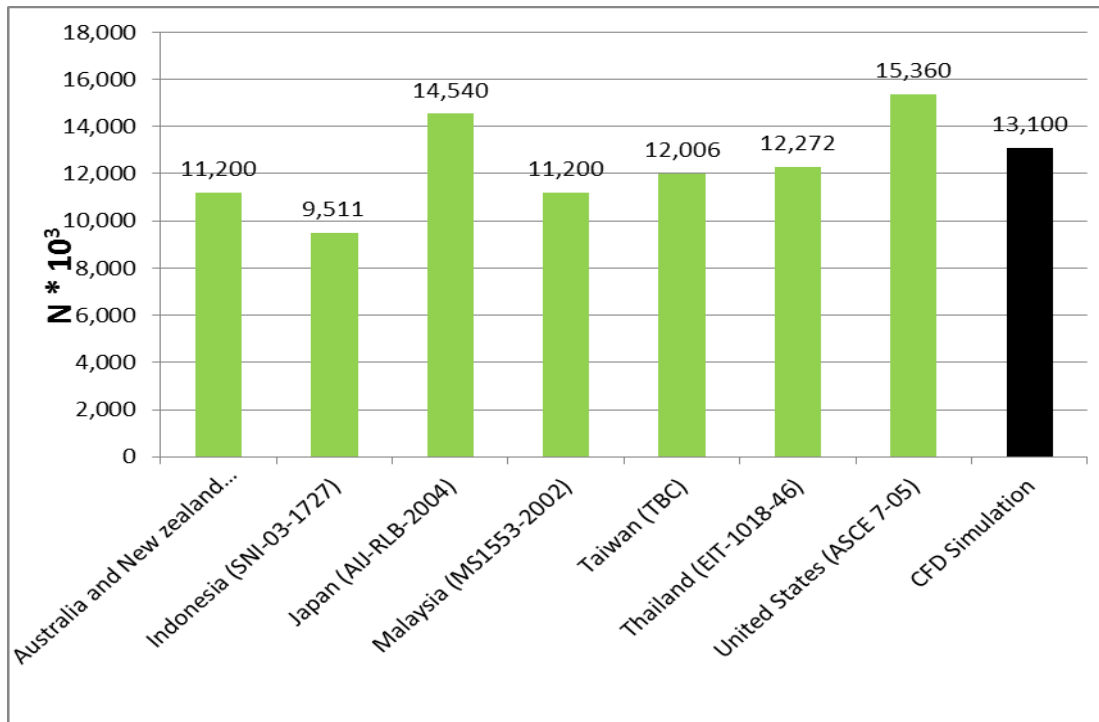


Figure 4.23 Base shear in the across wind direction by different codes and CFD Simulation

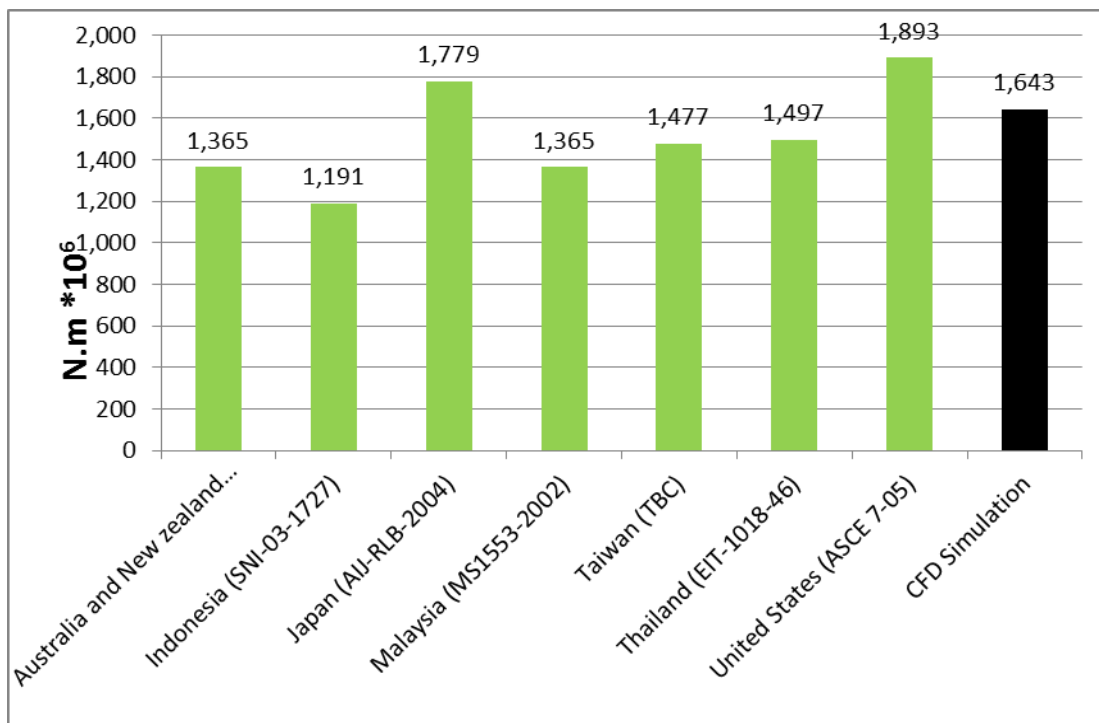


Figure 4.24 Base bending moment in the across wind direction by different codes and CFD Simulation

Figures 4.25 and 4.26 show the along wind base shear forces and the bending moments generated on the three building models studied in this investigation. As It is seen in the charts that the along wind shear forces for the building models with a single recession and a double recession have been recorded to be 83.76% and 83.4% of the model with no recessions, respectively. On the other hand, the base bending moments for single recession and double recession models have been observed to 81.32% and 80.7% of the rectangular model, respectively. A decrease of around 17% in base shear force and almost 20% in base bending moment is indispensable in structural design. However, it could be said that there is an insignificant difference between the building models with a single and a double recession, in terms of reduction in both the base shear force and the bending moment.

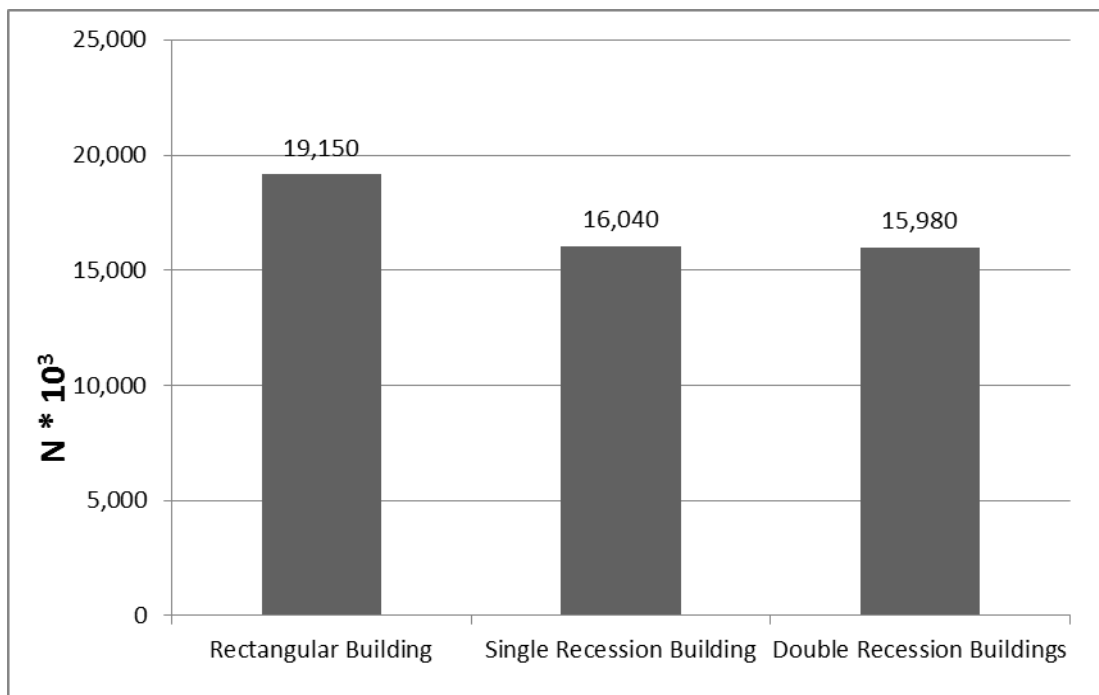


Figure 4.25 Base shear in the along wind direction different shapes of buildings by CFD Simulation

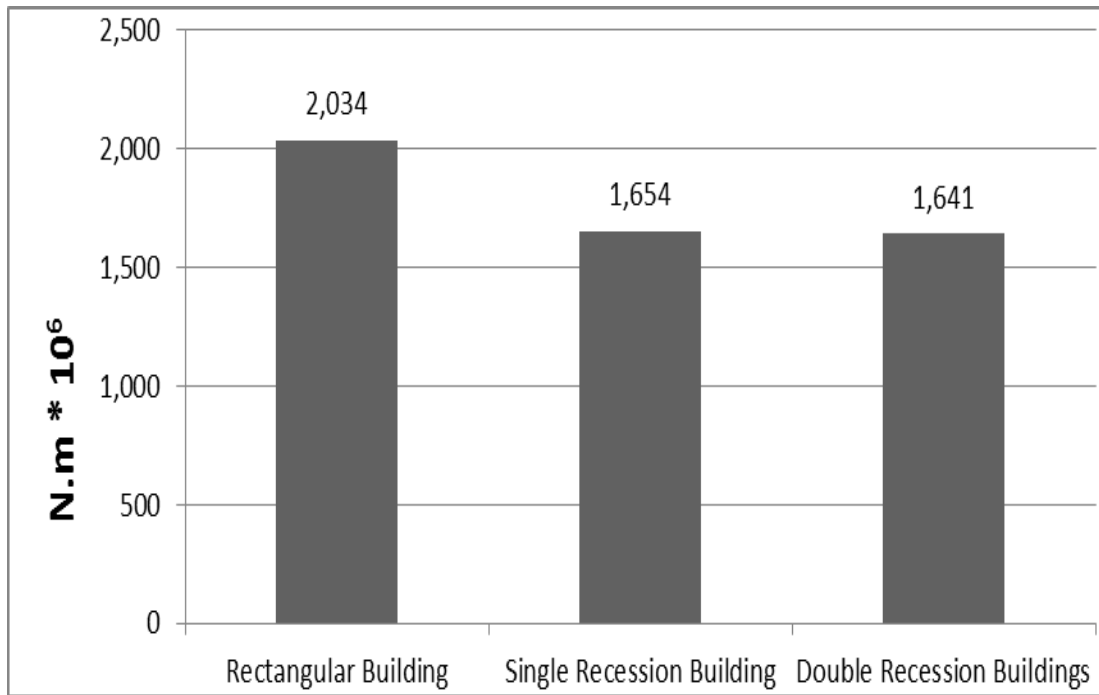


Figure 4.26 Base bending moment in the along wind direction different shapes of buildings by CFD Simulation

Figures 4.27 and 4.28 display the across wind base shear forces and the bending moments created on the three building models investigated in this study building. It can be perceived from the graphs that the across wind base shear force and the base bending moment in double recession model case is around 71.3% and 71.4% of the rectangular building model, respectively. While in single recession model the across wind base shear force was recorded to be 80.9% and the base bending moment was observed to be 81.6% of the results obtained for rectangular building model. Although, an insignificant difference was perceived between the building models with a single and a double recession in the along wind base shear forces and the bending moments, both the across wind base bending moment and the base shear force for the double recession model was observed to almost 12% less than that of the single recession model.

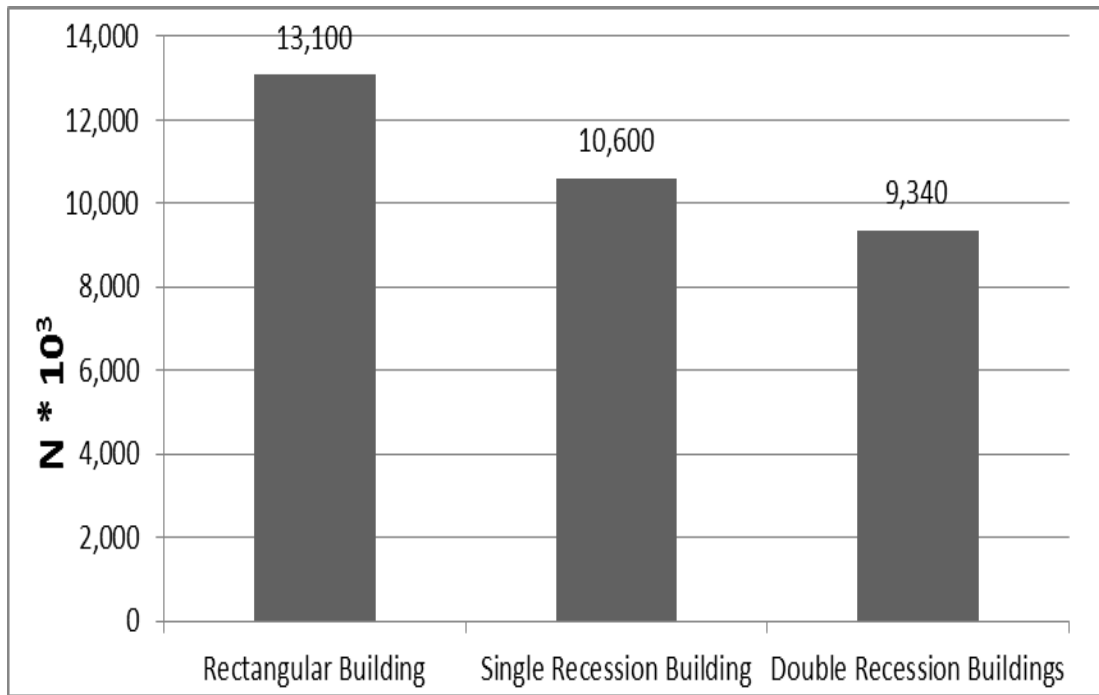


Figure 4.27 Base shear in the across wind direction different shapes of buildings by CFD Simulation

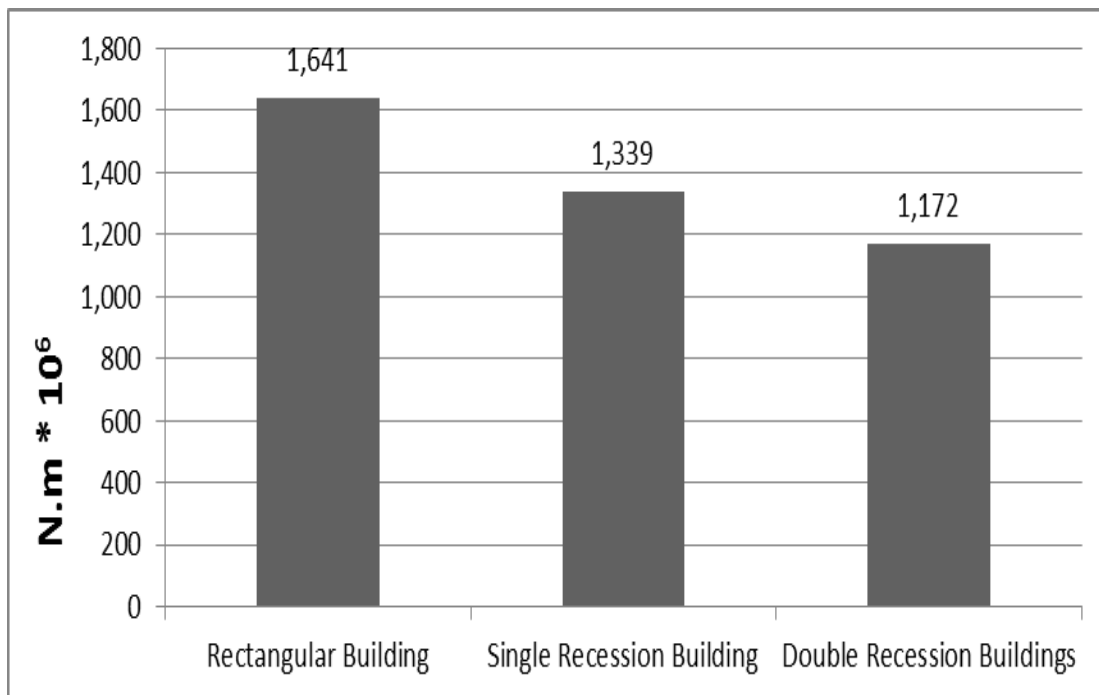


Figure 4.28 Base bending moment in across wind direction different shapes of buildings by CFD Simulation

CHAPTER 5

CONCLUSIONS

High-rise structures are subjected to vertical loads and horizontal loads. The vertical forces are consequence of the dead-weight of the building and the live load caused by furniture and people living or working in these structures. However, the horizontal forces are generated by wind or seismic loads. An isolated tall building model with three different plan area geometries have been numerically studied in this research, in order to determine the wind effect on high-rise structures. Under the action of wind flow, tall buildings oscillate simultaneously both in the direction of wind and perpendicular to the direction of wind. Numerical simulations were conducted by ANSYS FLUENT 14.0, which is commercially available computational fluid dynamic (CFD) software. The tests involved creating an incompressible turbulent boundary layer past the models and measuring wind pressures on the along wind and across wind faces of buildings. Realizable k- ϵ turbulence closure model, which is one of the most wide utilized models, was employed in the simulation analyses with wind velocity of 26 m/s.

The use of CFD codes enables design engineers to achieve precise results through numerical simulations. With the improvement of the turbulence closure models and computers, vortex shedding and the turbulence intensity could be predicted in a rigorous manner. Although wind tunnel tests produce more accurate results, they are cumbersome, time consuming and expensive compare to numerical methods.

In this study, three different building plan shapes with equal areas; basic rectangle, single corner-recession rectangle and double corner-recession rectangle were studied. The results obtained from the simulation analyses of basic rectangle shaped plan area building model were compared with a number of widely used codes and showed good agreement. Both the along wind and across wind base shear forces and base bending moments acting on the buildings were observed to be affected from the shape of the plan areas of the models. The values of these forces were noted to be the highest for the basic rectangle shape while they were lowest for the double corner-recession rectangle shape.

The along wind shear forces for the building models with a single and a double recession rectangle have been recorded to be 83.76% and 83.4% of the rectangle model with no recessions, respectively. On the other hand, the base bending moments for single recession rectangle and double recession rectangle models have been observed to 81.32% and 80.7% of the rectangular model, respectively. A decrease of around 17% in base shear forces and almost 20% in base bending moments is indispensable in structural design. However, it could be said that there is an insignificant difference between the building models with a single and a double recession, in terms of the reduction in base shear forces and the bending moments.

It can be perceived that the across wind base shear force and the base bending moment in double recession rectangular model case is around 71.3% and 71.4% of the basic rectangular building model, respectively. While in single recession rectangular model the across wind base shear force was recorded to be 80.9% and the base bending moment was observed to be 81.6% of the results obtained for simple rectangular building model. Although, an insignificant difference was perceived between the building models with a single and a double recessions in the along wind

base shear forces and the bending moments, both the across wind base bending moment and the base shear force for the double recession model was observed to almost 12% less than that of the single recession rectangular model.

REFERENCES

Armitt, J. (1980). Wind Loading on Cooling Towers, Journal of the Structural Division, **106**, No. 3, 623-641.

Baskaran, A., Stathopoulos, T. (1993). Numerical Computation of Wind Pressures on Buildings, Computers & Structures, **46**, No.6, 1029-1039.

Boggs, D., Hosoya, N., Cochran, L. (2000). Sources of torsional wind loading on tall buildings: Lessons from the wind tunnel, Structures Congress 2000: Advanced Technology in Structural Engineering, American Society of Civil Engineers, Reston, VA, 103.

Boussinesq, J. (1877). E Sur la Théorie des eaux Courantes, Mém. Prés. par Div. Savants à l' Acad.Sci.Paris, **23**, 1-680.

Campbell, Robert. (1995). Builder Faced Bigger Crisis than Falling Windows, Boston Globe. Boston, MA.

Cermak, J. E. (1977). Wind Tunnel Testing of Structures, Journal of the Engineering Mechanics Division of ASCE, **103**, 1125-1140.

Cermak, J. E. (1979). Applications of Wind Tunnels to Investigation of Wind Engineering Problems, Journal of American Institute of Aeronautics and Astronautics, **17**, 679-690.

Cermak, J. E. (1981). Wind Tunnel Design for Physical Modelling of Atmospheric Boundary Layer, Journal of the Engineering Mechanics Division of ASCE, **107**, 623-640.

Cermak, J. E. (1982). Physical Modelling of the Atmospheric Boundary Layer in Long Boundary Layer Wind Tunnels, Proc. Int. W/S on Wind Tunnel Modelling, USA, 97 -

125.

Cermak, J. E. (1984). Wind Simulation Criteria for Wind Effect Tests, *Journal of the Engineering Mechanics Division of ASCE*, **110**, 328-339.

Cermak, J. E. (1987). Advances for Physical Modelling for Wind Engineering, *Journal of the Engineering Mechanics Division of ASCE*, **113**, 737 -756.

Cermak, J. E. (1990). Atmospheric Boundary Layer Modelling in Wind Tunnels, Wind Loads on Structures, Int. Symposium, New Delhi, India, 3 -20.

Chen, X., and Kareem, A. (2005). Validity of Wind Load Distribution based on High Frequency Force Balance Measurements, *Journal of Structural Engineering of ASCE*, 984-987.

Counihan, J. (1969). An Improved Method of Simulating an Atmospheric Boundary Layer in a Wind Tunnel, *Journal of Atmospheric Environment*, **3**, 197-214.

Davenport, A.G. (1966). The treatment of wind loading on tall buildings, *Proceedings of a Symposium on Tall Buildings*, Pergamon Press, Southampton, 1-44.

Davenport, A. G. (1977). The prediction of risk under wind loading, *Proceedings in 2nd International Conference on Structure Safety and Reliability*, Munich, 511–538.

Davenport, A. G., Isyumov, N. (1967). The Application of the Boundary Layer Wind Tunnel to the Prediction of Wind Loading, *Proceedings of the 2nd International Conference on Wind Engineering*, Canada, Ottawa, 201-230.

Davenport, A. G. (1993b). How Can We Simplify and Generalize Wind Loads? , *Proceedings 3rd Asia-Pacific Symposium on Wind Engineering*, Hong Kong, **1**, 15 -26.

Davenport, A. G. (1998). What Makes A Structure Wind Sensitive? , *Wind Effects on Buildings and Structures*. Riera & Davenport (eds -1998) Balkema, Rotterdam, 1-13.

Djilali, N., Gartshore, I. S. (1992). Effect of leading-edge geometry on a turbulent Separation bubble, *American Institute of Aeronautics and Astronautics Journal*, **30(2)**, 559-561.

Ellingwood, B. R., Galambos, T., McGregor, J., and Cornell, C. A. (1980). Development of a probability based load criterion for American national standards A58, National Bureau of Standards, Washington, D.C.

Fujimoto, M., Ohkuma, T., and Amano, T. (1975). Dynamic Model Test of a High Rise Building in Wind Tunnel and in Natural Winds, *Proceedings of the 4th International Conference on Wind Engineering*, Heathrow, UK, 297-308.

Gairola, A., Upadhyay, A., and Kumar, K. (2006). Estimation of Wind Forces on A Memorial Structure, 3NCWE06_Kolkata, 139-151.

Germano, M., Piomelli, U., Moin, P. and Cabot, W.H. (1990). A Dynamic Sub grid-scale Eddy Viscosity Model, *Proceedings of the Summer Program, Centre for Turbulence Research, Stanford University*.

Gu, M., Zhou, Y., Xiang, H. F. (1999). Dynamic responses and equivalent wind loads of Jinmao Building, *Proceedings of the 10th International Conference on Wind Engineering*, Balkema, Rotterdam, pp. 1497-1504.

Hirt, C. W., Ramshaw, J. D., Stein, R. L. (1978). Numerical Simulation of Three-Dimensional Flow past Bluff Bodies, *Computer Methods in Applied Mechanics and Engineering*, **14, No.1**, 93-124.

Holmes, J. (2003). Emerging Issues in Wind Engineering, *Proceedings of the 11th International Conference on Wind Engineering*, 49-64.

Holmes, J. D. (2007). *Wind Loading of Structures (Second Edition)*, Taylor and Francis Group, New York.

Holmes, J., Rofail, A., Aurelius, L. (2003). High Frequency Base Balance Methodologies for Tall Buildings with Torsional and Coupled Resonant Modes, *Proceedings of the 11th International Conference on Wind Engineering*,

Holmes, J., Tamura Yukio, Krishna, Prem. (2008). Wind loads on low, medium and high-rise buildings by Asia-Pacific codes, The 4th International Conference on Advances in Wind and Structures, Jeju, Korea.

Islam, M. S., Ellingwood, B. and Corotis, R. B. (1990). Dynamic response of tall Buildings to stochastic wind load, *Journal of structural engineering of ASCE*, **116(11)**, 2982-3002.

Isyumov, N. (1982). The Aeroelastic Modelling of Tall Buildings, Proc. Int. W/S on Wind Tunnel Modelling, USA, 373 -407.

Isyumov, N., Steckley, A., Amin, N., and Fatehi, H. (1990). Effect of Orientation of the Principal Axis of Stiffness on the Dynamic Response of Slender Square Buildings *Journal of Wind Engineering and Industrial Aerodynamics*, **36**, 769-778.

Kareem, A. (1992). Dynamic Response of High Rise Buildings to Stochastic Wind Loads, *Journal of Wind Engineering and Industrial Aerodynamics*, (Proceedings of the 8th International Conference on Wind Engineering, Ontario, Canada), **41 -44**, 1101-1112.

Katagiri, J., Marukawa, H., Fujii, K., Nakamura, O., and Katsumura, A. (1995). Evaluation of Wind Responses of A Building Gained From Wind Tunnel Tests, *Proceedings of the 9th International Conference on Wind Engineering*, N. Delhi, India, 1408 -1419.

Kataoka, H. and Mizuno, M. (2002). Numerical Flow Computation around Aeroelastic 3D Square Cylinder Using Inflow Turbulence, *Journal of Wind and Structures*, **2-4**, 379-392.

Kwok, K.C.S. (1988). Effect of Building Shape on Wind Induced Response of Tall Buildings, *Journal of Wind Engineering and Industrial Aerodynamics*, **28**, 381-390.

Launder, B.E. and Kato, M. (1993). Modeling Flow-induced Oscillations in Turbulent Flow around Square Cylinder, American Society of Mechanical Engineers, Proc. Forum on Unsteady Flow (FED-Vol.157), 189.

Lee, S. (1997). Unsteady Aerodynamic Force Prediction on a Square Cylinder using k- ϵ Turbulence Models, Journal of Wind Engineering and Industrial Aerodynamics, **67-68**, No.6, 79-90.

LeMessurier, W. (1993). Breaking barriers, Magazine of Modern Steel Construction. **33**, No. 9, 26-33.

Lin, N., Letchford, C., Tamura, Y., Liang, Bo, Nakamura, O. (2005). Characteristics of wind forces acting on tall buildings, Journal of Wind Engineering and Industrial Aerodynamics, **93(3)**, 217-242.

Maruyama, T., Rodi, W., Maruyama, Y. and Hiraoka, H. (1999). Large Eddy Simulation of the Turbulent Boundary Layer behind Roughness Elements using an Artificially Generated Inflow, *Journal of Wind Engineering and Industrial Aerodynamics*, **83**, No.1-3, 381-392.

Mitra, D., and Kasperski, M. (2006). Determination of Appropriate Geometric Scale Ratio for Simulated Boundary Layer in Wind Tunnel, 3NCWE06_Kolkata, 104-112.

Murakami, S., Mochida, A. (1988). Three-dimensional Numerical Simulation of Airflow Around a Cubic Model by Means of k- ϵ model, Journal of Wind Engineering and Industrial Aerodynamics, **31**,283-303.

Murakami, S., Mochida, A. (1989). Three-dimensional Numerical Simulation of Turbulent Flow around Buildings Using the k- ϵ turbulence model, Journal of Building and Environment, **24**, 51-64.

Murakami, S. and Mochida, A. (1995). On Turbulent Vortex Shedding Flow Past 2D Square Cylinder Predicted by CFD, Journal of Wind Engineering and Industrial

Aerodynamics, **54**, 191-211.

Murakami, S. (1997). Current Status and Future Trends in Computational Wind Engineering, *Journal of Wind Engineering and Industrial Aerodynamics*, **67-68**, 3-34.

Nakayama, M., Ide, S.R., Sasaki, Y., and Tanaka, K. (1995). A Comparison of Wind Responses through Various Kinds of Wind Tunnel Techniques on a Super Tall Building, Proceedings of the 9th International Conference on Wind Engineering, N.Delhi, India, **1**, 346 -357.

Parera, M.D.A.E.S. (1978). A Wind Tunnel Study of the Interaction between Alongwind and Acrosswind Vibrations of Tall Slender Structures. *Journal of Wind Engineering and Industrial Aerodynamics*, **3**, 315-341.

Paterson, D. A., Apelt, C. J. (1986). Computation of Wind Flow over Three-dimensional Buildings, *Journal of Wind Engineering and Industrial Aerodynamics*, **24**, 192-213.

Peyrot, A. H., Saul, W.E., Jayachandran, P., and Tantichaiboriboon, V. (1974). Multi - degree Dynamic Analysis of Tall Buildings Subjected to Wind as a Stochastic Process, Proceedings of the Regional Conference on Tall Buildings, Bangkok, Thailand, 555 - 569.

Prandtl, L. (1921). Bermerkúngüber die Entststehung der Turbulenz, *Z. Angew. Math. Mech.*, **1**, 431-436.

Przulj, V. and Younis, B.A. (1993). Some Aspects of the Prediction of Turbulent Vortex Shedding from Bluff Bodies, American Society of Mechanical Engineering, **FED-Vol.149**, 75.

Rathbun, J.C. (1940). Wind Forces on a Tall Building, Transportation of American Society of Civil Engineers, **140**, 1 -82.

Reinhold, T.A. (1983). Distribution and Correlation of Dynamic Wind Loads, *Journal of the Engineering Mechanics Division of ASCE*, **109**, 1419 -1436.

Richards, D. (1966). Survey of aerodynamic problems in the electrical power supply industry, *Journal of the Royal Aerodynamic Society*, **70**.

Richards, P., Hoxey, R. (2004). Quasi-steady theory and point pressures on a cubic building, *Journal of Wind Engineering and Industrial Aerodynamics*, **92**, 1173-1190.

Roshko, A. (1993). Perspectives on bluff body aerodynamics, *Journal of Wind Engineering and Industrial Aerodynamics*, **49**, 79-100.

Sarvan Mamaidi, M.S. (2009). Analysis of a mini hydrokinetic turbine, Northern Illinois University.

Scott, R. (2001). In the Wake of Tacoma Suspension Bridges and the Quest for Aerodynamic Stability, ASCE. New York, NY.

Selvam, R. P. (1997). Computation of Pressures on TTU Building Using Large Eddy Simulation, *Journal of Wind Engineering and Industrial Aerodynamics*, **67-68**, 647-657.

Shih, T. H., Liou, W.W., Shabbir, A., Yang, Z., Zhu, J. (1995). A New Eddy-Viscosity Model for High Reynolds Number Turbulent Flows - Model Development and Validation, *Computers Fluids*, **24(3)**, 227-238.

Simiu, E. (1973a). Gust Factors and Alongwind Pressures Correlations, *Journal of Structural Engineering of ASCE*, **99**, 773-783.

Simiu, E. (1974b). Wind Spectra and Dynamic Alongwind Response, *Journal of Structural Engineering of ASCE*, **100**, 1897-1910.

Simiu, E. (1976). Equivalent Static Wind Loads for Tall Buildings Design, *Journal of Structural Engineering of ASCE*, **102**, 719-738.

Simiu, E. (1980). Revised Procedure for Estimating Alongwind Response, *Journal of Structural Engineering of ASCE*, **106**, 1-10.

Simiu, E. (1996). *Wind Effects on Structures (Third Edition)*, John Wiley and Sons, Inc., New York.

Solari, G. (1982). Alongwind Response Estimation: Closed Form Solution, *Journal of Structural Engineering of ASCE*, **108**, 225-240.

Solari, G. (1987b). Dynamic Alongwind Response of Structures by Response Spectrum Technique, *High Winds & Building Codes, WERC/NSF Sympo. on W.E., USA*, 445 - 452.

Song, C. C. S., He, J. (1993). Computation of Wind Flow around a Tall Building and the Large-Scale Vortex Structure, *Journal of Wind Engineering and Industrial Aerodynamics*, **46-47**, 219-228.

Steckley, A., Accardo, M., Gamble, S.L., Irwin, P.A., Williams, R.D. and Irwin, I., Guelph, O.C. (1992). The Use of Integrated Pressures to Determine Overall Wind-Induced Response, *Journal of Wind Engineering and Industrial Aerodynamics*, **41-44** 1023-1034.

Sutro, Dirk. (2000). Into the Tunnel, *Civil Engineering Magazine*.

Swaddiwudhipong, S., Khan, M. S. (2002). Dynamic Response of Wind-Excited Building Using CFD, *Journal of Sound and Vibration*, **253, No.4**, 735-754.

Taylor, Z., Palombi, E., Gurka, R., Kopp, G.A. (2011). Features of the turbulent flow around symmetric elongated bluff bodies, *Journal of Fluids and Structures*, **27**, 250-265.

Taylor, J. H. (2012). Numerical Simulation of a cross Flow Marine Hydrokinetic Turbine, Msc Thesis, Graduate School of Engineering of Washington University,

USA.

Vaicaitis, R., Shinozuka, M., and Takeno, M. (1975). Response Analysis of Tall Buildings to Wind Loading, *Journal of Structural Engineering of ASCE*, **101**, 585-600.

Vellozzi, J., Cohen, E. (1968). Gust Response Factors, *Journal of Structural Engineering of ASCE*, **94**, 1295-1313.

Vickery, B. J. (1971). On The Reliability of Gust Loading Factors, *Civil Engrg. Transactions, IEA, CE13 (1)*, 1-9.

Whitbread, R.E. (1963). Model Simulation of Wind Effects on Structures, *Proceedings of the 1st International Conference on Wind Engineering, NPL, England*, 284 -302.

Xie, J., Irwin, P.A., and Accardo, M. (1999). Wind Load Combinations for Structural Design of Tall Buildings, *Wind Engineering into the 21st Century, Larose & Livesey Balkema, Rotterdam*, 163-168.

Yang, J. N., Lin, Y.K. (1981). Alongwind Motion of Multi -Story Buildings, *Journal of the Engineering Mechanics of ASCE*, **107**, 295 -307.

Yoon, S. W., Ju, Y. K., Kim, S. B. (2003). Vibration Measurements of Tall Buildings in Korea, *Proceedings of the 11th International Conference on Wind Engineering*, 527-534.

APPENDIX A

```
#include "udf.h"

DEFINE_PROFILE (velocity_profile, t, i)
{
    real x[ND_ND];

    real y;

    face_t f;

    begin_f_loop (f, t)
    {
        F_CENTROID(x,f,t);

        y = x [1];

        F_PROFILE(f,t,i) = 26*pow(0.5*y,0.15);
    }
    end_f_loop (f,t)
}
```